Published in final edited form as:
J Comp Neurol. 2007 January 20; 500(3): 477–497. doi:10.1002/cne.21180.

Enriched Expression and Developmental Regulation of the Middle-Weight Neurofilament (*NF-M*) Gene in Song Control Nuclei of the Zebra Finch

TARCISO A.F. VELHO, **PETER LOVELL**, and **CLAUDIO V. MELLO***
Neurological Sciences Institute, Oregon Health and Science University, Beaverton, Oregon 97006

Abstract

Songbirds evolved a complex set of dimorphic telencephalic nuclei that are essential for the learning and production of song. These nuclei, which together make up the oscine song control system, present several neurochemical properties that distinguish them from the rest of the telencephalon. Here we show that the expression of the gene encoding the middle-weight neurofilament (*NF-M*), an important component of the neuronal cytoskeleton and a useful tool for studying the cytarchitectonic organization of mammalian cortical areas, is highly enriched in large neurons within pallial song control nuclei (nucleus HVC, robustus nucleus of the arcopallium, and lateral magnocellular nucleus of the nidopallium) of male zebra finches (*Taeniopygia guttata*). We also show that this transcript is highly expressed in large neurons in the medulla, pons, midbrain, and thalamus. Moreover, we demonstrate that *NF-M* expression in song control nuclei changes during postembryonic development, peaking during an early phase of the song-learning period that coincides with the maturation of the song system. We did not observe changes in *NF-M* expression in auditory areas or in song control nuclei in the contexts of hearing song or singing, although these contexts result in marked induction of the transcription factor ZENK. This observation suggests that *NF-M* might not be under the regulatory control of ZENK in auditory areas or in song control nuclei. Overall, our data indicate that *NF-M* is a neurochemical marker for pallial song control nuclei and provide suggestive evidence of an involvement of *NF-M* in the development and/or maturation of the oscine song control system.

Keywords

neurofilament; songbird; song development; vocal learning

Neurofilaments (NFs) are members of the intermediate filament protein family and are essential components of the neuronal cytoskeleton (for review see Lee and Cleveland, 1996). In the mammalian brain, NFs are particularly enriched in pyramidal neurons within cortical layers II/III, V, and VI and have been extensively used to help characterize the cytoarchitectonic organization of cortical areas (Hof et al., 1992, 1995; Chaudhuri et al.,

*Correspondence to: Claudio V. Mello, MD, PhD, Neurological Sciences Institute, Oregon Health and Science University, 505 NW 185th Ave., Beaverton, OR 97006. melloc@ohsu.edu.

1996; Hornung and Riederer, 1999; van der Gucht et al., 2001). In fact, based on regional variations of the laminar distribution of cells expressing NFs and other neurochemical markers, such as the calcium-binding proteins calbindin and calretinin, various species- and order-specific patterns of cortical organization have been identified (Hof and Sherwood, 2005). These patterns have proved very useful in defining degrees of taxonomic relatedness of cortical specializations across different mammalian species (Hof et al., 1992; Hof and Sherwood, 2005).

The expression of NFs has also been investigated in organisms such as goldfish, frogs, and chicken, but such studies have mostly focused on the retina, brainstem, and peripheral nervous system in the contexts of development and regeneration (Zopf et al., 1987; Glasgow et al., 1994; Gervasi and Szaro, 1997). A detailed account of the expression of NFs in the brain of a nonmammalian vertebrate species is therefore lacking. To address this gap, we have studied the expression of the gene encoding the middle-weight subunit of NF (*NF-M*), a major component of NF fibrils (Lee and Cleveland, 1996), in the brain of the zebra finch, a representative songbird species. Our main goal was to examine whether the analysis of expression of an NF gene would reveal regional neurochemical specializations of the avian brain, as occurs in mammals (Hornung and Riederer, 1999; Hof and Sherwood, 2005). Songbirds are of particular interest insofar as they represent one of only three avian orders (besides parrots and hummingbirds) that have evolved vocal learning (Nottebohm, 1972; Brenowitz et al., 1997a). Their brains contain a set of interconnected nuclei dedicated to vocal learning and production known as the *song control system* (Nottebohm and Arnold, 1976; Durand et al., 1997; Jarvis and Mello, 2000; Jarvis et al., 2000). Zebra finches, in particular, present a marked sexual dimorphism in their song control system (Nottebohm and Arnold, 1976) and have been the object of extensive neurobiological research (for reviews see Brenowitz et al., 1997b; Zeigler and Marler, 2004).

The song control system of songbirds can be divided into two main pathways. The direct vocal-motor pathway is required for song production (Nottebohm et al., 1976) and consists of the projections from nucleus HVC (we follow here the revised avian brain nomenclature; see Reiner et al., 2004) to the robust nucleus of the arcopallium (RA), and from RA to midbrain and medullary centers involved in the control of vocal and respiratory function (Nottebohm et al., 1982; for review see also Wild, 1997). The anterior forebrain pathway is required for vocal learning (Bottjer et al., 1984; Sohrabji et al., 1990; Scharff and Nottebohm, 1991) and consists of the projections from area X in the medial striatum to the medial part of the dorsolateral thalamic nucleus (DLM), from DLM to the lateral magnocellular nucleus of the anterior nidopallium (LMAN), and from LMAN back to area X (Bottjer et al., 1989; Vates et al., 1997; Luo et al., 2001). This anterior pathway is connected with nuclei in the direct motor pathway via HVC-to-X and LMAN-to-RA projections, and it is reminiscent of mammalian cortical-striatal-thalamic loops thought to be involved in the acquisition of movements requiring fine sequential sensorimotor integration (for review see Bottjer and Johnson, 1997). The nuclei in both pathways of the song control system can be easily identified by their distinct cytoarchitectonic features in Nissl-stained sections and by the differential expression of several markers related to specific hormonal, neurotransmitter, enzymatic, and transcription regulatory pathways (for examples, see the

reviews of Ball, 1994; Clayton, 1997). Such markers provide useful criteria for delineating the boundaries of individual song control nuclei. More important, though, is that they point to prominent neurochemical specializations of the song control system relative to the surrounding brain areas.

We report here that *NF-M* mRNA expression is highly enriched in song control nuclei HVC, LMAN, and RA and can therefore be a useful neurochemical marker for these brain areas. We also found that *NF-M* expression is significantly enriched in the primary thalamorecipient zones field L2 and nucleus basorostralis and in the globus pallidus, but it is relatively low and uniform throughout the remainder of the telencephalon. We show that the expression of *NF-M* is remarkably enriched in nuclei of the brainstem and diencephalon, most notably in several motor nuclei of cranial nerves and in some nuclei of the ascending auditory pathway. Throughout the brain, expression is most prominent in large neuronal cells that in several cases likely correspond to projection neurons. The observed expression pattern does not change acutely in response to auditory stimulation or in association with vocal behavior, indicating a constitutive expression of *NF-M* in brain areas associated with vocal communication in adults. This observation suggests that *NF-M* is not under the regulation of song-inducible transcription factors such as ZENK (also known aa zif-268, egr-1, NGFI-A, or krox-24) and c-Fos (Mello and Ribeiro, 1998; Bolhuis et al., 2000; Bailey and Wade, 2003). However, *NF-M* expression in song control nuclei varies with age and peaks during the early phase of the critical period for song learning, indicating a correlation between the regulated expression of *NF-M* and the early development of the song control system.

MATERIALS AND METHODS

NF-M cloning

PCR primers (forward-1: 5′aagctgctggagggtgaggagac3′; forward-2: 5′agctcgaggggctgaaacgaccg3′, reverse-1: 5′gggggatttagggggtgactttg3′) were designed based on conserved Rod, C1, and E domains within *NF-M* mRNA sequences from several species. Four extra primers (forward-3: 5′tgtcacaatagcatccaccaaaat3′, reverse-2: 5′ttttcatcctccaccttcgtctcttcaa3′, reverse-3: 5′tcctcagatacatccctccaacag3′, and reverse-4: 5′ctcttcagctttgctcttggc3′) were designed within the C1 and E domains from the sequence obtained with the initial PCR (forward-1 plus reverse-1) and within the 3′ untranslated region (UTR) from an ESTIMA library clone (SB02037B2C05 and GenBank accession No. DQ834450). Standard touchdown PCRs were performed with plasmid DNA extracted from a zebra finch brain cDNA library (Holzenberger et al., 1997; Denisenko-Nehrbass et al., 2000). All the amplified products were excised from an agarose gel, eluted with Qiagen's Gel Extraction Kit (Qiagen Inc., Valencia, CA), inserted into pPCRScript (Stratagene Inc., La Jolla, CA), and used to transform bacterial cells following standard procedures. Insert identity was confirmed by sequencing and analysis in DNAStar software (DNAStar Inc., Madison, WI).

Probe labeling

Riboprobes were used for in situ hybridization and Northern blot analyses. Plasmid DNA containing the cloned *NF-M* insert was isolated by using Qiagen's Miniprep Kit (Qiagen Inc.), linearized with the appropriate restriction enzymes, and purified with Qiagen's PCR Purification Kit (Qiagen Inc.). Sense and antisense ^{33}P-labeled riboprobes were synthesized as described elsewhere (Mello et al., 1997), purified in Sephadex G-50 columns, and quantified with a liquid scintillation counter.

Northern blot analysis

Total RNA from zebra finch adult brain was extracted via the Trizol method (Life Technologies Inc., Rockville, MD) and quantified by spectrophotometry. Ten micrograms of total RNA were separated by electrophoresis in 1% MOPS/formaldehyde agarose gel, and transferred with 10× SSC to nylon membranes (Hybond-N$^+$; Amersham Pharmacia Biotech Inc., Piscataway, NJ) as described in detail elsewhere (Mello et al., 1997). The membranes were incubated overnight in hybridization solution containing the ^{33}P-labeled antisense riboprobe (10^6 cpm/ml), followed by washes at 65°C and exposure to a Kodak storage phosphorscreen (Molecular Dynamics Inc., Sunnyvale, CA), which was read by a phosphorimager (Typhoon 8600; Molecular Dynamics Inc.).

Song stimulation and singing behavior

The birds used in this study (a total of 72 zebra finches, including adult males and females and juvenile males) were from our own breeding colony or were obtained from local breeders. For the song stimulation experiment, adult female zebra finches were isolated overnight (16–20 hours) in sound-attenuated chambers (~76 × 31 × 28 cm) under a 12:12-hour light:dark cycle (same as the aviary; lights on at 7:00 AM). On the following day, birds were exposed to a playback of a recorded conspecific song stimulus consisting of a medley of three representative nonfamiliar songs presented in blocks of 15 seconds followed by a 45-second silent interval. The birds were exposed to two stimulation protocols. In the first protocol (survival after onset series), birds heard the stimulus for 30 minutes and were killed after varying survival intervals (0.5, 2, 4, 6, and 8 hours) after stimulus onset. In the second protocol (stimulus duration series), birds heard the stimulus continually for increasing periods (0.5, 2, 4, 6, and 8 hours) and were killed immediately at the end of the stimulation. These two protocols are essentially as used by Velho et al. (2005). All stimuli were presented at comparable intensities (70 dB mean SPL at 35 cm from the speaker). Only females were used in this experiment, to avoid the confound of singing behavior; controls consisted of birds that were not stimulated. For analysis of singing behavior, males were first placed in acoustic isolation overnight and then monitored for singing behavior on the following morning after lights on, until death. Males that sang spontaneously were killed at 0.5 or 2 hours after singing started. Controls in this case consisted of birds that did not sing during the observation period (at least 2 hours after lights on). For the developmental study, we used juvenile males bred in our colony. In all cases, the sex was confirmed by direct post-mortem inspection of the gonads. All procedures involving birds were approved by OHSU's Institutional Animal Care Use Committee (IACUC) and are in accordance with NIH guidelines.

Tissue preparation

All birds were sacrificed by decapitation. Their brains were quickly dissected from the skull, frozen in Tissue-Tek (Sakura Finetek Inc., Torrance, CA) in a dry ice/isopropanol bath, and stored at −80°C. Parasagittal 10-μm brain sections were cut on a cryostat, thaw-mounted onto slides, and stored at −80°C until use.

Radioactive in situ hybridization

In situ hybridization (ISH) of serial parasagittal or frontal sections was performed by using ^{33}P-labelled sense and antisense riboprobes followed by phosphorimager autoradiography for a global assessment of *NF-M* mRNA distribution in the brain or emulsion autoradiography for various exposure durations and Nissl (cresyl violet or toluidine blue) counterstaining for regional and cellular levels of analysis. The hybridizations and washes were performed at 65°C, by using essentially the same procedure as previously described (Mello et al., 1997).

Densitometry

For quantitative analysis, brain sections from adults were chosen at levels where specific song control nuclei are well represented (approximately 1.5 mm lat for HVC and LMAN and 1.9 mm lat for RA). Sections were then selected from the brains of juveniles at levels containing the best (largest) representation of the equivalent nuclei. For NCM and L2a, sections from adult females at levels containing both areas (approximately 0.6 mm from the midline) were selected. All sections to be quantified were hybridized together in the same experiment. Phosphorimager autoradiograms were quantified in NIH Image. Densitometric measurements were taken over specific brain regions conservatively, by using a small window (about 300 μm^2) that respected the nuclear boundaries. The same window was used to measure song control nuclei and the adjacent regions (nidopallial shelf underneath HVC, arcopallial cup rostroventral to RA, and nidopallium immediately caudal to LMAN). After subtraction of slide background values, the measurements obtained from two adjacent sections were averaged for each area sampled. The resulting values were compared by ANOVA, followed by Fisher's PSDL posthoc tests for pairwise comparisons, with a probability of < 0.05 for significance.

Soma size estimates

We used Neurolucida software (MicroBrightField Inc., Colchester, VT) to draw the perimeters of individual neuronal somata positive and negative for *NF-M* in emulsion-dipped sections counterstained for Nissl and NeuroEx-plorer software (MicrobrightField Inc.) to derive the respective areas. We analyzed a 200-× 200-μm area within selected cytoarchitectonically defined regions from brain sections of at least three different animals ($n = 3–5$) and calculated the means and standard error of the estimated cell soma sizes. We also constructed frequency distribution histograms for different soma sizes. For area X, because of the low density of *NF-M*-positive cells, we measured the soma size of all labeled neurons within this nucleus for each section analyzed. We considered as neurons the cells containing a large, pale nucleus, usually with a clearly labeled nucleolus and strongly

labeled Nissl substance. In contrast, cells with a homogeneously and strongly labeled nucleus and scant cytoplasm were considered as glial.

Image acquisition and figure preparation

Images were acquired with a digital camera (DVC, Austin, TX) coupled to a Nikon E-600 microscope and a PC using Neurolucida software (MicroBrightField Inc.). Adobe Photoshop (Adobe, San Jose, CA) was used to assemble photomicrograph plates and for adjustments in brightness and contrast of both photomicrographs and phosphorimager autoradiograms. For preparation of emulsion autoradiogram figures, the amount of exposure was optimized for each nucleus to result in clearly labeled cells without obscuring cellular morphology; as a consequence, the density of grains over cells is not directly comparable across figures, unless noted otherwise. For Figure 12, the autoradiograms were color-coded in NIH Image.

RESULTS

Cloning of the zebra finch homologue of *NF-M*

To obtain the zebra finch homologue of *NF-M*, we identified conserved domains in previously cloned avian and mammalian (canary, chicken, and mouse) homologues, and designed primers to amplify a 564-bp fragment within the coding region of *NF-M* from a zebra finch brain cDNA library. The predicted amino acid sequence of the amplified fragment (GenBank accession No. AY494949) spanned residues 400–583 of the chicken *NF-M* gene (GenBank accession No. X17102; Zopf et al., 1987; Fig. 1A,B), starting at the 3′ end of the highly conserved Rod domain and ending at the beginning of the repeats (R) domain, thus including the whole conserved domain 1 (C1) and the glutamate-enriched region (E) of the *NF-M* gene (top black bar in Fig. 1A). The ISH data presented here were obtained primarily with probes derived from this clone. We have also identified a 492-bp cDNA from the ESTIMA consortium database (clone SB02037B2C05; http://titan.biotec.uiuc.edu/cgi-bin/ESTWebsite/estima_start?seqSet=songbird; GenBank accession No. DQ834450) that represents the 3′ UTR of *NF-M* (Fig. 1A) and that shows 86.6% identity with the chicken homologue. This clone yielded essentially the same expression patterns by ISH as our primary probe. To obtain further sequence for *NF-M*, we designed primers at the beginning of the Rod domain and at the 3′ UTR, in combination with primers based on the E and C1 domains. We obtained two PCR products that overlapped with each other and with the initial fragment covering the C1 and E domains as well as an additional product that includes the entire Rod domain and the beginning of the C1 domain (black bars in Fig. 1A; GenBank accession No. DQ834451). The predicted amino acid sequence derived from the combined amplified fragments spanned residues 107–858, from the beginning of the Rod domain until the carboxy-terminal end of the protein. The combined zebra finch sequence had overall identities of 89.4%, 73.5%, and 72.5% at the nucleotide level and 91.1%, 71.5%, and 68.5% at the aminoacid level with the chicken, mouse, and human *NF-M* homologues, respectively. Notably, the zebra finch sequence showed only 85.6% and 86.6% identity at the nucleotide and protein levels, respectively, with a partial cDNA clone representing canary *NF-M* (GenBank accession No. AF053711). A possible explanation is that a large portion of the canary sequence consists of the more variable E domain.

A close inspection revealed, as expected, that the sequences in the Rod, C1, and C2 domains are highly conserved across species, whereas the E and R domains are more variable (Fig. 1B). For example, the sequences in avian species lack some glutamate-rich sequences shared by the mouse and human homologues. A 30-amino-acid region within the R domain is also missing in birds. Within the R domain, two consensus phosphorylation sites represented by lysine-serine-proline (KSP) motifs were found in the zebra finch sequence (Fig. 1B, asterisks). A Northern blot analysis of zebra finch total telencephalic mRNA hybridized with a riboprobe from the C1/E domain revealed a single band of ~3.8 kb (see Fig. 3C). This is consistent with the expected size of the *NF-M* gene based on the chicken homologue and demonstrates the specificity of our riboprobe. We have also identified through a blast search an ~1,200-bp cDNA from the ESTIMA database (clone SB02025B2F01), which was shown, based on sequence analysis, to represent the 3′ end of the light-weight neurofilament gene (*NF-L*; 83.5% and 70.6% homology at the nucleotide level with chicken and human sequences, respectively).

NF-M expression: global pattern

The general brain distribution of *NF-M* mRNA was studied by radioactive ISH of serial parasagittal (Fig. 2) and frontal (Fig. 3) sections from adult male zebra finches. The most conspicuous feature of *NF-M* expression on autoradiograms was the highly enriched expression in various discrete regions of the brainstem, which emulsion analysis showed to correspond to specific nuclei in the medulla, pons, midbrain, and thalamus (see below). In contrast, *NF-M* expression was relatively low and uniform throughout the telencephalon, with the exception of discrete areas of highly enriched expression corresponding to some nuclei of the song control system and part of the globus pallidus (GP). A less marked but still prominent enrichment of expression was seen in telencephalic thalamorecipient zones. A semiquantitative analysis of relative expression levels for all brain structures examined is shown in Table 1. At the cellular level, based on emulsion-dipped slides, *NF-M* was clearly expressed in neuronal cells, with an overall tendency for higher expression in larger cells. The labeling often had a perinuclear distribution, indicating a predominantly somatic localization of the transcript. In contrast, *NF-M* expression was conspicuously absent in glial cells, laminae, fiber tracts, ventricular zone, and choroid plexus. Specific examples of cellullar labeling are included in the figures concerning regional *NF-M* expression. Hybridization with sense strand riboprobes (Fig. 2F) performed in parallel with antisense probes (Fig. 2E) did not yield any detectable signal, demonstrating probe specificity (see also Fig. 5G-J).

To determine whether the general expression pattern observed for *NF-M* was unique to this transcript or was also shared with other neurofilament genes, we examined the *NF-L* by using a probe from the identified zebra finch homologue. We observed essentially the same pattern as for *NF-M*, including the enriched expression in nuclei of the hindbrain, midbrain, and thalamus (Fig. 2A′) and the highly enriched expression in telencephalic song control nuclei (Fig. 2C′); no signal was detected upon hybridization with the sense strand probe. Thus, *NF-M* and *NF-L* have very similar general expression patterns in the zebra finch brain. Throughout the remainder of this paper, we present a detailed regional analysis of *NF-M* expression.

NF-M expression: hindbrain, midbrain and thalamus

Close to the midline, *NF-M* expression was most conspicuous in discrete nuclei of the dorsal midbrain, as clearly seen on parasagittal sections (Fig. 2A; see also frontal section shown in Fig. 3B). The regions of highest expression corresponded to the dorsal and ventral subdivisions of the oculomotor nucleus (OMd and OMv) and the nucleus of the trochlear nerve (NIV; Figs. 2A, 3B, 4B,C), all of which were characterized by very large neurons containing very high densities of emulsion grains. A somewhat lower expression was seen dorsocaudally to OMd, in the relatively smaller neurons of the nucleus of Edinger-Westphal (EW). *NF-M* expression was also very conspicuous in the large neurons of the motor nucleus of the trigeminal nerve (MNV; Fig. 4D) and in several large neuronal cells scattered throughout the medial reticular formation in the medulla (not shown). Markedly high expression of *NF-M* was also seen in the epithalamus, corresponding to the medial and lateral habenular nuclei (HB; Figs. 2A, 3A, 4E,F; note the lack of expression in the choroid plexus), although a small domain lacking *NF-M* expression was present in the dorsal part of the lateral habenular nucleus (not shown).

At a slightly more lateral level (Fig. 2B), *NF-M* expression was conspicuously high in discrete areas of the dorsal pons that corresponded to cochlear nuclei. Both nucleus magnocellularis (NM) and its target nucleus laminaris (LM) showed very high expression throughout their extension (Fig. 5B,C). A relatively lower but still marked expression in comparison with the surrounds was seen in thalamic areas corresponding to nucleus ovoidalis (Ov) in the auditory pathway and DLM in the anterior forebrain pathway of the song system (Fig. 5E,F). Expression in DLM was most conspicuous in the large cells of the core and less marked in the shell region. In the cerebellum, *NF-M* expression was markedly enriched in the deep nuclei and in the Purkinje cell layer (Fig. 5D). Although hybridization with the antisense strand riboprobe resulted in a high accumulation of emulsion grains over the large neuronal cells typical of nuclei such as NM (Fig. 5G) and DN (Fig. 5I), hybridization with the sense strand riboprobe did not result in any detectable signal in these nuclei (Fig. 5H,J, respectively) or in any other nuclei, demonstrating probe specificity at the cellular level. More laterally (Figs. 2C, 3), *NF-M* expression was very high in thalamic nucleus rotundus as well as in several other discrete nuclei containing large neuronal cells in the pons and medulla, whose identity we have not determined. Large neuronal cells with high *NF-M* expression could also be seen scattered throughout the lateral pons and medulla (not shown). Highly enriched expression of *NF-M* was also seen in some layers of the optic tectum and in the magnocellular division of the isthmic nucleus (IM; Figs. 2D, 3; details not shown).

NF-M expression: telencephalon

The most conspicuous feature of *NF-M* expression in the telencephalon was its high enrichment in all the pallial nuclei of the song control system, in sharp contrast to the surrounding areas (Figs. 2C, 3). Emulsion autoradiography analysis revealed that high *NF-M* expression in the caudodorsal nidopallium is confined within the boundaries of song nucleus HVC as defined by cytoarchitectonic criteria based on Nissl staining (Figs. 2C, 3A, 6A,B). A closer inspection showed that *NF-M* expression in HVC was highest in large neurons (Fig. 6C, large arrows), which most likely represent area X-projecting cells (Alvarez-Buylla et al.,

1988), whereas smaller neurons, which often occur in the periphery of the clusters characteristic of HVC and likely represent RA-projecting cells or interneurons, showed much lower or no expression (Fig 6C, small arrows). In medial parasagittal sections, a small region in the dorsocaudal nidopallium corresponding to a medial extension of HVC, i.e., the para-HVC region (Foster and Bottjer, 1998), also showed enriched expression in comparison with the adjacent NCM (Fig 6B, inset).

In the rostral nidopallium, the region of enriched *NF-M* expression corresponded to song nucleus LMAN (Figs. 2C, 7A,B). A close inspection of LMAN's core region, which has large neuronal cells and can be readily identified based on cytoarchitectonic criteria (Fig. 7A), revealed that *NF-M* expression is highly enriched in large neurons (Fig. 7C, large arrows), while smaller neuronal cells tended to have much lower or no expression (Fig. 7C, small arrows). Cells with high *NF-M* expression were not confined to LMAN's core, though, but also occurred at a lower density in the LMAN *shell* region (Fig. 7A,B), most prominently in the caudal domain. An examination of serial frontal sections revealed that *NF-M* is also relatively enriched in MMAN (Fig. 7D,E). The labeling pattern in MMAN resembled that of other previously described neurochemical markers for this nucleus (Nastiuk and Clayton, 1995; Holzenberger et al., 1997; Akutagawa and Konishi, 2001) but was spatially more restricted than MMAN as defined based on cytoarchitectonics and connectivity (see Figs. 2, 7 in Vates et al., 1997).

In the arcopallium, the area of highest *NF-M* expression (Figs. 2C, 3B) corresponded to song nucleus RA, as defined by cytoarchitectonic criteria upon Nissl staining and as clearly visualized under darkfield illumination (Fig. 8A,B). At the cellular level, the large neuronal cells characteristic of RA expressed high levels of *NF-M* (Fig. 8C, large arrows), whereas smaller neurons likely consisting of interneurons exhibited very low or no expression (Fig. 8C, small arrows). In addition, as clearly seen in frontal sections, a somewhat less enriched zone extended laterally beyond RA into an arc-like domain (Figs. 3B, 8B) that seems to correspond to the dorsal arcopallium (Ad) as defined previously by connectivity and neurochemical criteria (Johnson et al., 1995; Bottjer et al., 2000).

Within the basal ganglia, *NF-M* expression was most highly enriched in the caudal part of the globus pallidus (Figs. 2C, 9A,B), where the typical large neuronal cells showed very high densities of emulsion grains (Fig. 9C, arrows). In striatal song nucleus area X (Fig. 9D-F), although the large majority of cells showed low or no expression of *NF-M*, several large and widely spaced neurons had a very high accumulation of emulsion grains (Fig. 9E,F, arrows). The overall expression in area X did not differ, however, from the general pattern in the striatum, so that there was no appreciable enhancement of expression in area X over its surrounds (Fig. 2C).

Another telencephalic area with a prominent enrichment of *NF-M* expression was the auditory thalamorecipient zone field L2a, in comparison with the caudomedial nidopallium (NCM) and mesopallium (CMM; Figs. 2B,C, 10A-C). Although L2a has a higher cell density than its surrounds, the enhanced expression of *NF-M* was clearly attributable to a higher expression (grain density) over individual cells in L2a (Fig. 10E) than in NCM (Fig. 10D) or in CMM (not shown). At this medial brain level, a discrete domain of enriched

expression was also seen in the caudodorsal hippocampus (Fig. 10A). This appears to correspond to a discrete nucleus recognizable upon Nissl staining as a cluster of relatively large cells immediately adjacent to the dorsal edge of the brain (Fig. 10F-H). *NF-M* expression was also enriched rostrally in the somatosensory-recipient nucleus basorostralis, owing to both an overall higher density of grains over cells and a more frequent occurrence of individual large cells with a very high grain density, in comparison with adjacent areas such as the rostral striatum (Fig. 10I,J). The visual thalamorecipient zone entopallium showed a less prominent but recognizable enrichment in comparison with its surrounds (Fig. 2D; details not shown). Finally, a slight but noticeable enrichment of expression compared with the adjacent nidopallium was seen in song nucleus interface (NIf; not shown, but see below).

Developmental regulation of *NF-M* expression

The song control system undergoes extensive changes in cellular and molecular properties during the critical period for song learning (Alvarez-Buylla and Kirn, 1997; Clayton, 1997). We therefore examined *NF-M* expression in song control nuclei of juvenile males, to test for a possible regulation during postembryonic development and/or in conjunction with song learning. We found a highly enriched expression in all pallial song nuclei at all ages examined [posthatch days (phd) 15, 20, 35, 50, and >120; Fig. 12A].

A densitometric analysis (n = 5 adults and 3 juveniles per age analyzed) revealed an effect of age on all pallial song control nuclei. In HVC, *NF-M* expression differed significantly across ages [ANOVA, $F(1051.7) = 4.074$, $P = 0.02$], peaking on phd 50 and declining thereafter (Fig. 12B, white columns; Fisher's PLSD, $P = 0.007$, $P = 0.005$, and $P = 0.01$ for phd 20, phd 35, and adults, respectively, compared with phd 50). In contrast, the adjacent nidopallial shelf region showed no significant differences across ages [Fig. 12B, gray columns; $F(94.01) = 1.085$, $P = 0.41$]. Already by phd 20, *NF-M* expression in HVC was associated with large neuronal cells (Fig. 12C).

A significant effect of age on *NF-M* expression was also seen in LMAN [ANOVA, $F(914.372) = 4.074$, $P = 0.032$], where expression levels increased progressively, reaching a peak on phd 35 and declining thereafter (Fig. 12C, white columns). Post hoc comparisons showed significantly higher expression on phd 35 compared with phd 15 and with adults (Fisher's PLSD, $P = 0.028$ and $P = 0.008$, respectively) and a significantly lower expression in adults compared with all other age groups, with the exception of phd 15 (Fisher's PLSD, $P = 0.016$, $P = 0.008$, and $P = 0.034$ for phd 20, 35, and 50, respectively). In contrast, the signal in the nidopallium caudal to LMAN showed no significant differences across ages [Fig. 12C, gray columns; $F(94.038) = 1.35$, $P = 0.3181$ by ANOVA], demonstrating the anatomical specificity of the effect seen in LMAN.

NF-M expression in RA also increased with age, peaking on phd 35 and declining subsequently to adult levels (Fig. 12D, white columns). The effect of age was significant [$F(2099) = 4.156$ $P = 0.03$ by ANOVA], and post hoc analysis showed significantly higher expression on phd 35 compared with phd 15 and adults (Fisher's PLSD, $P = 0.02$ and $P = 0.0038$, respectively) and significantly lower expression in adults than on phd 20 (Fisher's PLSD, $P = 0.026$). In contrast, the adjacent arcopallial cup area showed no significant

variation across ages [Fig. 12D, gray columns; F(61.4) = 0.726, *P* = 0.6 by ANOVA]. The expression in RA was also associated with large neuronal cells on phd 20 (Fig. 13D,E). *NF-M* expression in NIf was very marked on phd 35, seen as a high accumulation of grains over individual cells in this nucleus (Fig. 13F,G), an effect that was more noticeable than in adults (not shown).

Soma size estimates

Our cellular analysis suggested a correlation between neuronal size and the expression levels of *NF-M* (and of *NF-L*), particularly in regions of highly enriched expression. To obtain further evidence in this regard, we estimated the soma size of *NF-M* positive (*NF-M*$^+$) and negative (*NF-M*$^-$) neurons in selected brain areas (Fig. 11). Our results revealed that the size distributions for *NF-M*$^+$ and *NF-M*$^-$ neurons are significantly different, with little overlap, in song nuclei HVC, LMAN, RA, and area × (Kolmogorov–Smirnov test, $p < 0.0001$ for all song nuclei; Fig. 11A-D). In contrast, with L2a and the hippocampus, areas that showed more moderate *NF-M* expression, these two categories of neurons showed highly overlapping size distributions (Kolmogorov–Smirnov test, $p = 0.0729$ for L2a and $p = 0.59$ for Hp; Fig. 11E and F).

NF-M expression in females

We also examined the pattern of *NF-M* expression in brain sections of adult female zebra finches. We observed that females (Fig. 14A-C) show essentially the same pattern as males, most particularly the highly enriched expression in specific nuclei of the brainstem, such as the DLM, DN, and NM. More importantly, we also observed an enriched expression in the telencephalic song nuclei, namely, HVC, LMAN, and RA (Fig. 14D-F). Because these nuclei are small in females, they are hard to visualize in the phosphorimager autoradiograms, but the emulsion analysis showed a clear enrichment of expression compared with the surrounding areas.

Lack of *NF-M* regulation by neuronal activation

The zinc-finger transcription factor ZENK (also known as zif-268, egr-1, NGFI-A, or krox-24) is inducible in auditory areas such as NCM and CMM by song stimulation (Mello et al., 1992) and in song control nuclei in the context of singing behavior (Jarvis and Nottebohm, 1997). We have examined the promoter region of the chicken and human *NF-M* homologues (GenBank accession Nos. X17102 and S46954, respectively) and in both cases detected the presence of a consensus ZENK binding site (Christy and Nathans, 1989; Knapska and Kaczmarek, 2004), suggesting that this gene might be under ZENK regulation. We therefore examined whether *NF-M* expression might be regulated in auditory areas by song stimulation or in song nuclei by singing behavior. However, we did not observe any apparent effects on inspection of autoradiograms. A densitometric analysis confirmed a lack of significant changes in *NF-M* expression in NCM and L2a of birds stimulated for 30 minutes and sacrificed after various survival intervals [ANOVA, F(0.14) = 2.191, *P* = 0.39, and F(0.122) = 1.421, *P* = 0.25, for NCM and L2a, respectively; n = 3–5 per group] and in birds stimulated for various periods of time [F(0.054) = 1.415, *P* = 0.25, and F(0.12) = 0.203, *P* = 0.95, for NCM and L2a, respectively; n = 3–5 per group] compared with

unstimulated controls. Similarly, no significant changes were seen in HVC, LMAN, and RA of actively singing birds sacrificed at 0.5 and 2 hours after onset of singing behavior, compared with quiet controls [ANOVA, $F(10.313) = 0.189$, $P = 0.83$; $F(419.9) = 1.03$, $P = 0.42$; and $F(275.8) = 1.44$, $P = 0.32$, respectively; n = 3 per group].

DISCUSSION

In the present study, we analyzed the expression of the middle-weight neurofilament (*NF-M*), a member of the intermediate filament family, in the zebra finch brain using in situ hybridization. We found that the *NF-M* transcript is highly enriched in various nuclei located in several brain subdivisions. The expression is most often associated with large neuronal cells that resemble long-range projection neurons, although some exceptions were noted. Most importantly, we show that *NF-M* expression is highly enriched in the pallial nuclei of the song control system and that significant changes in expression levels occur in these nuclei during a period that overlaps with the early phase of the critical period for song learning. We discuss below the relevance of our findings.

NF-M expression is prominent in large neurons

Throughout the brain, cellular analysis shows a high expression of *NF-M* in large neuronal cells, often with a characteristic perinuclear pattern suggesting a primarily somatic localization. In contrast, expression is low in small neurons and essentially lacking in glial and ependymal cells. This correlation with neuronal size is consistent with the presumed role of *NF-M* as a major determinant of the caliber and conduction velocity of axonal fibers and with its requirement in the maintenance of large myelinated axons (Yamasaki et al., 1992; Kure and Brown, 1995; Elder et al., 1999a,b). We observed particularly high expression in several sensory and motor nuclei of cranial nerves and in some thalamic nuclei, all of which are typically constituted by large long-range and/or multipolar projection neurons. In addition, for the song control system, we specifically demonstrate that cells that express *NF-M* are, on average, 2.5–3 times larger than cells that do not express the gene (see Fig. 11). Although we did not utilize combined tract tracing and in situ analysis, previous studies have shown that the large cells present in song nuclei HVC and RA are typically projection neurons (Dutar et al., 1998; Spiro et al., 1999). An enrichment of neurofilament expression in large neuronal cells seems to be a general characteristic of vertebrates, insofar as it has been observed in all species examined to date, including frogs, chickens, quails, and primates (Zopf et al., 1987; Yamasaki et al., 1992; Sakaguchi et al., 1993; Chaudhuri et al., 1996; Zhao and Szaro, 1997). A correlation with neuronal size was not ubiquitous, however; medium-sized to large neurons in parts of the telencephalon (e.g., the hippocampus) and diencephalon of the zebra finch did not show enriched expression. In addition, L2a, which contains smaller cells than its targets NCM and CMM, showed higher grain density per cell in comparison with these adjacent structures. Thus, cell size is an important but not the sole determinant of *NF-M* expression levels in brain cells.

NF-M enrichment in the song control system

The most prominent feature of *NF-M* expression in the telencephalon is its marked enrichment in the pallial song control nuclei (HVC, LMAN, and RA). This pattern is not the

result of a trivial effect such as a difference in cell density between song nuclei and their surroundings. In fact, we have shown that this transcript is enriched in the large neuronal cells characteristic of song nuclei, in comparison with adjacent areas and the rest of the telencephalon, where expression is uniformly low. Our data thus provide further evidence for the neurochemical specialization of the oscine song control system. The enrichment of *NF-M* expression in song nuclei was seen both in males and in females, although for the latter a quantitative analysis was not performed.

Previous studies have identified specializations of this system based on the differential expression or binding density of ligands related to sex steroid and neurotransmitter receptors, neuromodulators and peptides, growth factors, and activity-induced transcription factors (George and Clayton, 1992; Ball, 1994; Bottjer and Alexander, 1995; George et al., 1995; Mello and Clayton, 1995; Nastiuk and Clayton, 1995; Holzenberger et al., 1997; Gahr and Metzdorf, 1999; Metzdorf et al., 1999; Denisenko-Nehrbass et al., 2000; Riters and Ball, 2002; Haesler et al., 2004; Sockman et al., 2004; Teramitsu et al., 2004; Wada et al., 2004). Our present data extend this phenomenon to an important component of the neuronal cytoskeleton. Intriguingly, some of these markers, namely, the androgen receptor (AR), the retinoic acid-generating enzyme zRalDH, the antigen SNAg, and the cannabinoid receptor (CB1), share significant similarities with the *NF-M* pattern reported here (Denisenko-Nehrbass et al., 2000; Akutagawa and Konishi, 2001; Soderstrom et al., 2004) but also show important differences. CB1, for example, is enriched in all telencephalic song nuclei, including striatal area X, and appears to be expressed mainly in small neurons. AR and zRalDH, on the other hand, are enriched only in adult HVC and LMAN, but not in RA, and are also expressed in larger neuronal cells (X-projecting HVC cells in the case of zRalDH). Although at present a causal relationship cannot be derived, androgen has marked trophic effects on target cells within song nuclei, affecting several morphological traits such as soma size, size and complexity of dendritic branches, and density of axonal projections (Gurney, 1981; Canady et al., 1988; Schlinger and Arnold, 1991). Because of its association with neuronal cell size, *NF-M* expression could partially reflect some of the known androgen actions.

In marked contrast to the pallial song nuclei, *NF-M* expression is not enriched in striatal area X. For the latter, we observed that a discrete number of large cells with high *NF-M* expression are interspersed with numerous smaller cells showing low or no expression. An interesting possibility, based on our size estimate for these cells ($177.3 \pm 5.7\ \mu m^2$ soma area), is that they may correspond to some of the largest γ-aminobutyric acid (GABA)-ergic neurons that participate in the projection from area X to DLM in the thalamus ($148 \pm 37\ \mu m^2$; Luo and Perkel, 1999). It should be stressed, however, that the *NF-M* expression pattern observed in area X appears to be a general characteristic of the striatum rather than a peculiarity of area X.

NF-M expression was also enriched in an arc-like region lateral to RA within the arcopallium. This region appears to correspond to the Ad area shown to receive a projection from the shell region that surrounds LMAN [Johnson et al., 1995; Bottjer, 2004; not to be confused with the dorsal arcopallium (AD) as defined by Reiner et al., 2004] and that may be part of a system of topographically organized projections parallel to the main projections

of the song control system. Although the precise function of this parallel system and its possible relation with song learning is unclear, it is interesting to note that *NF-M* also appears to be expressed in the LMAN shell. In addition, some neurochemical markers of RA, such as the AR and the α2-subunit of the adrenergic receptor, also label Ad (Balthazart et al., 1992; Riters and Ball, 2002), suggesting an intriguing relationship between the song control system and these parallel pathways.

NF-M expression patterns: comparison with other birds

Several features of the regional distribution of *NF-M* expression in the zebra finch brain are similar to those seen in other avian species, such as quail and chicken, including the high level of expression in some thalamic nuclei, portions of the optic tectum, cranial nerve nuclei, and Purkinje cells and deep nuclei in the cerebellum (Zopf et al., 1987; Yamasaki et al., 1992; Ohara et al., 1993). In contrast, our present study is the first to describe in detail the distribution of a neurofilament-encoding mRNA in the telencephalon of an avian species. We have also obtained preliminary evidence that *NF-M* expression in canaries is similar to that described here for zebra finches, including the enrichment in the brainstem and in song control nuclei. Nevertheless, it is at present unclear whether the enriched expression of *NF-M* in pallial song nuclei is unique to songbirds or extends to other avian vocal learner orders (i.e., parrots and hummingbirds), as occurs to some extent for AR and the NR2A subunit of the N-methyl-D-aspartate (NMDA) receptor (Gahr, 2000; Wada et al., 2004). It will also be interesting to determine whether the expression of *NF-M* and other neurofilament genes reveals specializations in nonlearner avian groups, which lack distinct pallial vocal control nuclei based on cytoarchitectonics and the differential expression of markers such as AR and glutamate receptor subtypes (Karten and Hodos, 1967; Kuenzel and Masson, 1988; Kroodsma and Konishi, 1991; Gahr, 2000; Wada et al., 2004).

NF-M expression: comparison with mammals

Specific data on *NF-M* mRNA expression in the brainstem are lacking in mammals. However, the brain distribution of the neurofilament light gene (*NF-L*) mRNA has been described for mice (Kure and Brown, 1995). Although *NF-M* and *NF-L* are two distinct genes, they are usually thought to be coexpressed, because functional neurofilament fibrils consist of heteropolymers containing the proteins encoded by the *NF-L* plus either the *NF-M* or the *NF-H* (neurofilament heavy) genes, most commonly both of the latter (Elder et al., 1999b). Indeed, these three polypeptides have highly overlapping expression patterns in rats (Trojanowski et al., 1986). Moreover, we have observed a close resemblance in the expression patterns of *NF-M* and *NF-L* in zebra finches. In mice, intense *NF-L* expression is associated with large neuronal cells in various nuclei throughout the diencephalon and mesencephalon and in specific parts of the cerebellum, namely, the Purkinje cell layer and deep nuclei (Kure and Brown, 1995), in a pattern that closely resembles the distribution of *NF-M* (and *NF-L*) in the zebra finch. These observations suggest that the distribution of neurofilament transcripts is conserved at the level of the brainstem and thalamus.

A comparison of telencephalic patterns between birds and mammals requires further caution. First, most studies examining the morphology and regional and laminar distributions of neurofilament-expressing cortical neurons have relied on ICC (Hof et al.,

1992; Chaudhuri et al., 1996; Hornung and Riederer, 1999; Boire et al., 2005; Hof and Sherwood, 2005). There is, however, a general agreement between the known distributions of cells expressing *NF-L* mRNA and neurofilament protein in rodents (Kure and Brown, 1995; Hornung and Riederer, 1999; Boire et al., 2005), suggesting that in situ patterns are a reasonable predictor of the distribution of somata positive for neurofilament protein. Second, because the avian telencephalon lacks, for the most part, a corticolaminar organization, it is less clear where the specific homologies lie. It has recently been recognized, however, that most of the avian telencephalon consists of pallial domains that are distinct from basal ganglia and that can be considered homologous, as a whole, to mammalian cortical regions (Reiner et al., 2004; Jarvis et al., 2005). Moreover, the avian pallium contains distinct sensory thalamorecipient zones that project to specific telencephalic targets (e.g., field L2a and its targets NCM and CMM in the auditory system; Karten, 1968; Kelley and Nottebohm, 1979; Wild et al., 1993; Vates et al., 1996). Based on such criteria, these primary and second-order telencephalic areas can be thought of as equivalent to thalamorecipient layers and supragranular targets in the respective cortical areas (Karten and Shimizu, 1989; Karten, 1997; for alternative views see Jarvis et al., 2005). Finally, it is unclear whether birds have multiple areas equivalent to the various cortical representations subserving a particular sensory modality (Medina and Reiner, 2000; Kaas and Collins, 2001), so some important aspects of the regional distribution of *NF-M* cannot be currently verified in birds.

In spite of the constraints described above, a general characteristic of the mammalian cortex is that the thalamorecipient layer (layer IV within sensory, motor, and association areas) is mainly devoid of NF-expressing cells, whereas supragranular and infragranular layers (layers II–III and V, respectively) have high densities of such cells (Hornung and Riederer, 1999). This is clearly distinct from the pattern we observed in zebra finches, wherein the auditory thalamorecipient field L2a exhibits higher *NF-M* expression than its adjacent supragranular-like targets NCM and CMM. A similar but less pronounced enrichment is also evident in the primary target areas for visual and trigeminal inputs (respectively the entopallium and n. basorostralis) in comparison with their surrounds. Thus, the regional/laminar distributions of neurofilament do not appear to be conserved at the telencephalic level between birds and mammals.

Lack of *NF-M* regulation by neuronal activation

Our data demonstrate that *NF-M* expression is not regulated in the zebra finch brain by song stimulation or singing behavior, conditions known to lead to the robust induction of genes encoding activity-dependent transcription factors, such as *zenk, c-fos*, and *c-jun*, in auditory and song control areas (Mello et al., 1992; Mello and Clayton, 1994; Nastiuk et al., 1994; Jarvis and Nottebohm, 1997; Kimpo and Doupe, 1997; Bolhuis et al., 2000; Bailey and Wade, 2003; Sockman et al., 2004; Velho et al., 2005). These data suggest that *NF-M* is not regulated by ZENK or other song-induced transcription factor in the zebra finch, in spite of the fact that a ZENK/Egr-1 canonical binding site is present in the chicken and human *NF-M* promoters (Velho and Mello, unpublished observations). A possible explanation is that ZENK might not have ready access to the *NF-M* promoter in these brain areas because of epigenetic factors such as the state of methylation of the promoter, as is the case for the

glucocorticoid receptor, a known ZENK/Egr-1 target in the rat (Weaver et al., 2004). In addition, one cannot exclude the possibility that ZENK might have a negative regulatory effect on *NF-M* expression. That possibility might explain, for example, the high expression of *NF-M* at sites lacking ZENK expression, such as field L2a and the entopallium, and the low expression of *NF-M* in an area of high ZENK expression, such as NCM. At any rate, we have not observed any evidence of *NF-M* regulation in the present study.

Developmental regulation of *NF-M* expression

Our data demonstrate that *NF-M* is already markedly enriched in all pallial song nuclei in juveniles by phd 15. At this age, a large proportion of RA-projecting cells has not yet been incorporated into HVC (Alvarez-Buylla et al., 1988), and the connection between HVC and RA is largely absent (Konishi and Akutagawa, 1985), suggesting that the HVC neurons expressing high levels of *NF-M* are mainly X-projecting neurons. This is consistent with the morphological characteristics of the *NF-M*-expressing neurons in both juveniles and adults and the enriched expression in the para-HVC region of adults, which lacks RA-projecting neurons (Foster and Bottjer, 1998).

NF-M expression in both LMAN and RA increases and peaks early (phd 35), whereas the increase within HVC occurs later (phd 50) during the song learning period, which in zebra finches extends from about phd 25 (beginning of the sensory acquisition phase) to phd 90 (end of the sensorimotor phase; Immelmann, 1969; Price, 1979; Eales, 1985, 1987; Bohner, 1990; Clayton, 1997; for review see White, 2001). During the time of peak *NF-M* expression, important changes occur in the song system, particularly the establishment of the HVC-to-RA projection and the marked cellular growth and neuronal death within individual song nuclei (Bottjer et al., 1985, 1986; Konishi and Akutagawa, 1985, 1990). LMAN, for instance, undergoes marked neuronal loss that results in a size reduction that is complete by phd 37 (Korsia and Bottjer, 1989). This reduction, however, is not accompanied by an increase in the density of any specific neuronal subpopulation (Korsia and Bottjer, 1989). Thus, the increase in *NF-M* signal in LMAN of juveniles most likely reflects an increase in the relative amount of transcript in individual remaining neurons. Moreover, between phd 20 and 35, the main efferent projection of LMAN (LMAN-to-RA) undergoes marked pruning of terminals and rearrangement of existing synapses (Iyengar et al., 1999). Thus, even though the cells in the LMAN-to-RA projection are being reduced in number, the up-regulation of *NF-M* in LMAN somata during this period could be associated with the maturation (e.g., an increase in axonal caliber) of the remaining fibers in this projection.

The observed changes in *NF-M* expression in RA also seem to occur in parallel with cytoarchitectonic changes in this nucleus during development. By phd 15, RA is indistinguishable between males and females, but, as the birds age further, RA regresses markedly in females and grows in males (Konishi and Akutagawa, 1985). In fact, the soma size of RA neurons increases with a time course similar to that we observed for *NF-M* mRNA expression, with a peak at phd 35 and a slight decrease in adults (Konishi and Akutagawa, 1985). Because the growth in soma and neuropil is accompanied by a decrease in overall cell density, the increase in overall *NF-M* expression in RA most likely is due to an increase in mRNA levels within individual cells. During the same period, the young

males are making early attempts to produce their own song, which potentially requires the strengthening and maturation of the projections from RA to its midbrain and medullary targets.

The developmental regulation of *NF-M* expression could also be associated with changes known to occur in other neurochemical properties of the song system. Most fundamentally, the growth and maturation of the song control system are under the strong regulatory action of sex steroids (Gurney, 1981; Konishi and Akutagawa, 1985; Schlinger and Arnold, 1991; Simpson and Vicario, 1991). In female zebra finches, for example, RA and HVC neurons grow to sizes similar to those of males upon administration of estrogen (Konishi and Akutagawa, 1985). We have observed that the promoter region of the chicken *NF-M* gene contains at least one consensus estrogen-responsive element (ERE) half-site next to a possible nonconsensus half-site, and in close proximity to an Sp1 binding site (not shown), suggesting a possible regulatory role of estrogens in *NF-M* expression. Significant developmental increases also occur in the modulatory tonus of cholinergic and catecholaminergic inputs and in the expression of brain-derived growth factor (BDNF) in the song system (Sakaguchi and Saito, 1989, 1991; Akutagawa and Konishi, 1998). The expression of both chicken and rat *NF-M* is up-regulated in neuronal cells upon treatment with neurotrophic factors (Verge et al., 1990; Zopf et al., 1990). Moreover, the expression of BDNF in the brain of juvenile zebra finches shows regional and temporal changes similar to those we describe here for *NF-M* (Akutagawa and Konishi, 1998), raising the possibility that BDNF might be involved in the regulation of *NF-M* expression. Finally, the developmental changes we observed in *NF-M* expression might be associated with the auditory experience and/or changes in singing behavior that juveniles experience during the song-learning period. The lack of *NF-M* regulation by song stimulation and singing that we observed in adults argues against this possibility, but further studies in juveniles will be required to settle the issue.

In sum, our study has identified several conserved features of *NF-M* expression and demonstrated its enrichment in telencephalic nuclei that are specialized for the acquisition and production of learned vocalizations. These results add a structural protein to a list of neurochemical specializations that reflect the unique properties of the oscine song control system. *NF-M* expression in song nuclei changes markedly during ontogeny, peaking at an early phase of the vocal learning period, when important changes in the song system and in singing behavior are taking place. Future developmental and comparative studies of *NF-M* and other neurofilaments in vocal learner and nonlearner groups should give further insights into the relationship between this neurochemical specialization and the biology of vocal learning and associated brain circuits.

Acknowledgments

We thank Jin Kwong Jeong for help with animal handling and histological preparations and two anonymous reviewers for their insightful comments on the manuscript.

Grant sponsor: National Institute of Deafness and Other Communication Disorders; Grant number: DC02853.

Abbreviations

A	arcopallium
Ad	dorsal arcopallium
Bas	nucleus basorostralis
Cb	cerebellum
CMM	caudomedial mesopallium
CP	posterior commissure
DLM	medial part of the dorsolateral thalamic nucleus
DN	deep cerebellar nuclei
E	entopallium
EW	Edinger-Westphal nucleus
FLM	medial longitudinal fasciculus
GCT	central gray substance
gl	cerebellar granule cell layer
GP	globus pallidus
H	hyperpallium
HB	habenular nuclei
Hp	hippocampus
HVC	nucleus HVC of the nidopallium
IM	magnocellular division of the isthmic nucleus
L1	subfield L1 of field L
L2a	subfield L2a of field L
L3	subfield L3 of field L
LMAN	lateral magnocellular nucleus of the anterior nidopallium
M	mesopallium
ml	cerebellar molecular layer
MLd	dorsal part of the lateral mesencephalic nucleus
MMAN	medial magnocellular nucleus of the anterior nidopallium
MN V	motor nucleus of the trigeminal nerve
N	nidopallium
NC	caudal nidopallium
NCM	caudomedial nidopallium

NIII	oculomotor nerve
NIV	nucleus of the trochear nerve
NL	nucleus laminaris
NIf	nucleus interface of the nidopallium
NM	nucleus magnocellularis
OMd	dorsal part of the oculomotor nerve nucleus
OMv	ventral part of the oculomotor nerve nucleus
OT	optic tract
Ov	nucleus ovoidalis
PC	choroid plexus
pcl	cerebellar Purkinje cell layer
Pt	nucleus pretectalis
RA	robust nucleus of the arcopallium
Rt	nucleus rotundus
S	septum
St	striatum
TeO	optic tectum
X	area X of the medial striatum

LITERATURE CITED

Akutagawa E, Konishi M. Transient expression and transport of brain-derived neurotrophic factor in the male zebra finch's song system during vocal development. Proc Natl Acad Sci U S A. 1998; 95:11429–11434. [PubMed: 9736753]

Akutagawa E, Konishi M. A monoclonal antibody specific to a song system nuclear antigen in estrildine finches. Neuron. 2001; 31:545–556. [PubMed: 11545714]

Alvarez-Buylla A, Kirn JR. Birth, migration, incorporation, and death of vocal control neurons in adult songbirds. J Neurobiol. 1997; 33:585–601. [PubMed: 9369461]

Alvarez-Buylla A, Theelen M, Nottebohm F. Mapping of radial glia and of a new cell type in adult canary brain. J Neurosci. 1988; 8:2707–2712. [PubMed: 3411349]

Bailey DJ, Wade J. Differential expression of the immediate early genes FOS and ZENK following auditory stimulation in the juvenile male and female zebra finch. Brain Res Mol Brain Res. 2003; 116:147–154. [PubMed: 12941470]

Ball GF. Neurochemical specializations associated with vocal learning and production in songbirds and budgerigars. Brain Behav Evol. 1994; 44:234–246. [PubMed: 7842283]

Balthazart J, Foidart A, Wilson EM, Ball GF. Immunocytochemical localization of androgen receptors in the male songbird and quail brain. J Comp Neurol. 1992; 317:407–420. [PubMed: 1578004]

Bohner J. Early acquisition of song in the zebra finch, *Taeniopygia guttata*. Anim Behav. 1990; 39:369–374.

Boire D, Desgent S, Matteau I, Ptito M. Regional analysis of neurofilament protein immunoreactivity in the hamster's cortex. J Chem Neuroanat. 2005; 29:193–208. [PubMed: 15820621]

Bolhuis JJ, Zijlstra GG, den Boer-Visser AM, Van Der Zee EA. Localized neuronal activation in the zebra finch brain is related to the strength of song learning. Proc Natl Acad Sci U S A. 2000; 97:2282–2285. [PubMed: 10681421]

Bottjer SW. Developmental regulation of basal ganglia circuitry during the sensitive period for vocal learning in songbirds. Ann N Y Acad Sci. 2004; 1016:395–415. [PubMed: 15313787]

Bottjer SW, Alexander G. Localization of met-enkephalin and vasoactive intestinal polypeptide in the brains of male zebra finches. Brain Behav Evol. 1995; 45:153–177. [PubMed: 7796094]

Bottjer SW, Johnson F. Circuits, hormones, and learning: vocal behavior in songbirds. J Neurobiol. 1997; 33:602–618. [PubMed: 9369462]

Bottjer SW, Miesner EA, Arnold AP. Forebrain lesions disrupt development but not maintenance of song in passerine birds. Science. 1984; 224:901–903. [PubMed: 6719123]

Bottjer SW, Glaessner SL, Arnold AP. Ontogeny of brain nuclei controlling song learning and behavior in zebra finches. J Neurosci. 1985; 5:1556–1562. [PubMed: 4009245]

Bottjer SW, Miesner EA, Arnold AP. Changes in neuronal number, density and size account for increases in volume of song-control nuclei during song development in zebra finches. Neurosci Lett. 1986; 67:263–268. [PubMed: 3737014]

Bottjer SW, Halsema KA, Brown SA, Miesner EA. Axonal connections of a forebrain nucleus involved with vocal learning in zebra finches. J Comp Neurol. 1989; 279:312–326. [PubMed: 2464011]

Bottjer SW, Brady JD, Cribbs B. Connections of a motor cortical region in zebra finches: relation to pathways for vocal learning. J Comp Neurol. 2000; 420:244–260. [PubMed: 10753310]

Brenowitz EA, Margoliash D, Nordeen KW. An introduction to birdsong and the avian song system. J Neurobiol. 1997a; 33:495–500. [PubMed: 9369455]

Brenowitz EA, Margoliash D, Nordeen KW. The neurobiology of birdsong. J Neurobiol. 1997b; 33:495–710. [PubMed: 9369455]

Canady RA, Burd GD, DeVoogd TJ, Nottebohm F. Effect of testosterone on input received by an identified neuron type of the canary song system: a Golgi/electron microscopy/degeneration study. J Neurosci. 1988; 8:3770–3784. [PubMed: 2461435]

Chaudhuri A, Zangenehpour S, Matsubara JA, Cynader MS. Differential expression of neurofilament protein in the visual system of the vervet monkey. Brain Res. 1996; 709:17–26. [PubMed: 8869552]

Christy B, Nathans D. DNA binding site of the growth factor-inducible protein Zif268. Proc Natl Acad Sci U S A. 1989; 86:8737–8741. [PubMed: 2510170]

Clayton DF. Role of gene regulation in song circuit development and song learning. J Neurobiol. 1997; 33:549–571. [PubMed: 9369459]

Denisenko-Nehrbass NI, Jarvis E, Scharff C, Nottebohm F, Mello CV. Site-specific retinoic acid production in the brain of adult songbirds. Neuron. 2000; 27:359–370. [PubMed: 10985355]

Durand SE, Heaton JT, Amateau SK, Brauth SE. Vocal control pathways through the anterior forebrain of a parrot (*Melopsittacus undulatus*). J Comp Neurol. 1997; 377:179–206. [PubMed: 8986880]

Dutar P, Vu HM, Perkel DJ. Multiple cell types distinguished by physiological, pharmacological, and anatomic properties in nucleus HVc of the adult zebra finch. J Neurophysiol. 1998; 80:1828–1838. [PubMed: 9772242]

Eales LA. Song learning in zebra finches: some effects of song model availability on what is learnt and when. Anim Behav. 1985; 33:1293–1300.

Eales LA. Song learning in female-raised zebra finchs: another look at the sensitive phase. Anim Behav. 1987; 35:1356–1365.

Elder GA, Friedrich VL Jr, Margita A, Lazzarini RA. Age-related atrophy of motor axons in mice deficient in the mid-sized neurofilament subunit. J Cell Biol. 1999a; 146:181–192. [PubMed: 10402469]

Elder GA, Friedrich VL Jr, Pereira D, Tu PH, Zhang B, Lee VM, Lazzarini RA. Mice with disrupted midsized and heavy neurofilament genes lack axonal neurofilaments but have unaltered numbers of axonal microtubules. J Neurosci Res. 1999b; 57:23–32. [PubMed: 10397632]

Foster EF, Bottjer SW. Axonal connections of the high vocal center and surrounding cortical regions in juvenile and adult male zebra finches. J Comp Neurol. 1998; 397:118–138. [PubMed: 9671283]

Gahr M. Neural song control system of hummingbirds: comparison to swifts, vocal learning (songbirds) and nonlearning (suboscines) passerines, and vocal learning (budgerigars) and nonlearning (dove, owl, gull, quail, chicken) nonpasserines. J Comp Neurol. 2000; 426:182–196. [PubMed: 10982462]

Gahr M, Metzdorf R. The sexually dimorphic expression of androgen receptors in the song nucleus hyperstriatalis ventrale pars caudale of the zebra finch develops independently of gonadal steroids. J Neurosci. 1999; 19:2628–2636. [PubMed: 10087076]

George JM, Clayton DF. Differential regulation in the avian song control circuit of an mRNA predicting a highly conserved protein related to protein kinase C and the bcr oncogene. Brain Res Mol Brain Res. 1992; 12:323–329. [PubMed: 1374499]

George JM, Jin H, Woods WS, Clayton DF. Characterization of a novel protein regulated during the critical period for song learning in the zebra finch. Neuron. 1995; 15:361–372. [PubMed: 7646890]

Gervasi C, Szaro BG. Sequence and expression patterns of two forms of the middle molecular weight neurofilament protein (*NF-M*) of *Xenopus laevis*. Brain Res Mol Brain Res. 1997; 48:229–242. [PubMed: 9332720]

Glasgow E, Hall CM, Schechter N. Organization, sequence, and expression of a gene encoding goldfish neurofilament medium protein. J Neurochem. 1994; 63:52–61. [PubMed: 8207446]

Gurney ME. Hormonal control of cell form and number in the zebra finch song system. J Neurosci. 1981; 1:658–673. [PubMed: 7346574]

Haesler S, Wada K, Nshdejan A, Morrisey EE, Lints T, Jarvis ED, Scharff C. FoxP2 expression in avian vocal learners and nonlearners. J Neurosci. 2004; 24:3164–3175. [PubMed: 15056696]

Hof PR, Sherwood CC. Morphomolecular neuronal phenotypes in the neocortex reflect phylogenetic relationships among certain mammalian orders. Anat Rec A Discov Mol Cell Evol Biol. 2005; 287:1153–1163. [PubMed: 16211636]

Hof PR, Glezer II, Archin N, Janssen WG, Morgane PJ, Morrison JH. The primary auditory cortex in cetacean and human brain: a comparative analysis of neurofilament protein-containing pyramidal neurons. Neurosci Lett. 1992; 146:91–95. [PubMed: 1475055]

Hof PR, Nimchinsky EA, Morrison JH. Neurochemical phenotype of corticocortical connections in the macaque monkey: quantitative analysis of a subset of neurofilament protein-immunoreactive projection neurons in frontal, parietal, temporal, and cingulate cortices. J Comp Neurol. 1995; 362:109–133. [PubMed: 8576425]

Holzenberger M, Jarvis ED, Chong C, Grossman M, Nottebohm F, Scharff C. Selective expression of insulin-like growth factor II in the songbird brain. J Neurosci. 1997; 17:6974–6987. [PubMed: 9278533]

Hornung JP, Riederer BM. Medium-sized neurofilament protein related to maturation of a subset of cortical neurons. J Comp Neurol. 1999; 414:348–360. [PubMed: 10516601]

Immelmann, K. Song development in the zebra finch and other estrilid finches. In: Hinde, RA., editor. Bird vocalizations. Cambridge University Press; Cambridge: 1969. p. 61-74.

Iyengar S, Viswanathan SS, Bottjer SW. Development of topography within song control circuitry of zebra finches during the sensitive period for song learning. J Neurosci. 1999; 19:6037–6057. [PubMed: 10407041]

Jarvis ED, Mello CV. Molecular mapping of brain areas involved in parrot vocal communication. J Comp Neurol. 2000; 419:1–31. [PubMed: 10717637]

Jarvis ED, Nottebohm F. Motor-driven gene expression. Proc Natl Acad Sci U S A. 1997; 94:4097–4102. [PubMed: 9108111]

Jarvis ED, Ribeiro S, da Silva ML, Ventura D, Vielliard J, Mello CV. Behaviourally driven gene expression reveals song nuclei in hummingbird brain. Nature. 2000; 406:628–632. [PubMed: 10949303]

Jarvis ED, Gunturkun O, Bruce L, Csillag A, Karten H, Kuenzel W, Medina L, Paxinos G, Perkel DJ, Shimizu T, Striedter G, Wild JM, Ball GF, Dugas-Ford J, Durand SE, Hough GE, Husband S, Kubikova L, Lee DW, Mello CV, Powers A, Siang C, Smulders TV, Wada K, White SA,

Yamamoto K, Yu J, Reiner A, Butler AB. Avian brains and a new understanding of vertebrate brain evolution. Nat Rev Neurosci. 2005; 6:151–159. [PubMed: 15685220]

Johnson F, Sablan MM, Bottjer SW. Topographic organization of a forebrain pathway involved with vocal learning in zebra finches. J Comp Neurol. 1995; 358:260–278. [PubMed: 7560286]

Kaas JH, Collins CE. The organization of sensory cortex. Curr Opin Neurobiol. 2001; 11:498–504. [PubMed: 11502398]

Karten HJ. The ascending auditory pathway in the pigeon (*Columba livia*). II. Telencephalic projections of the nucleus ovoidalis thalami. Brain Res. 1968; 11:134–153. [PubMed: 5749228]

Karten HJ. Evolutionary developmental biology meets the brain: the origins of mammalian cortex. Proc Natl Acad Sci U S A. 1997; 94:2800–2804. [PubMed: 9096300]

Karten, HJ.; Hodos, W. A stereotaxic atlas of the brain of the pigeon (*Columba livia*). Johns Hopkins Press; Baltimore, MD: 1967.

Karten HJ, Shimizu T. The origins of neocortex: connections and lamination as distinct events in evolution. J Cogn Neurosci. 1989; 1:291–301. [PubMed: 23971981]

Kelley DB, Nottebohm F. Projections of a telencephalic auditory nucleus—field L—in the canary. J Comp Neurol. 1979; 183:455–469. [PubMed: 759444]

Kimpo RR, Doupe AJ. FOS is induced by singing in distinct neuronal populations in a motor network. Neuron. 1997; 18:315–325. [PubMed: 9052801]

Knapska E, Kaczmarek L. A gene for neuronal plasticity in the mammalian brain: Zif268/Egr-1/NGFI-A/Krox-24/TIS8/ZENK? Prog Neurobiol. 2004; 74:183–211. [PubMed: 15556287]

Konishi M, Akutagawa E. Neuronal growth, atrophy and death in a sexually dimorphic song nucleus in the zebra finch brain. Nature. 1985; 315:145–147. [PubMed: 3990816]

Konishi M, Akutagawa E. Growth and atrophy of neurons labeled at their birth in a song nucleus of the zebra finch. Proc Natl Acad Sci U S A. 1990; 87:3538–3541. [PubMed: 2333299]

Korsia S, Bottjer SW. Developmental changes in the cellular composition of a brain nucleus involved with song learning in zebra finches. Neuron. 1989; 3:451–460. [PubMed: 2561972]

Kroodsma DE, Konishi M. A suboscine bird (eastern phoebe, *Sayornis phoebe*) develops normal song without auditory feedback. Anim Behav. 1991; 42:477–487.

Kuenzel, WJ.; Masson, M. A stereotaxic atlas of the brain of the chick (*Gallus domesticus*). Johns Hopkins University Press; Baltimore, MD: 1988.

Kure R, Brown IR. Expression of low-molecular-weight neurofilament (*NF-L*) mRNA during postnatal development of the mouse brain. Neurochem Res. 1995; 20:833–846. [PubMed: 7477677]

Lee MK, Cleveland DW. Neuronal intermediate filaments. Annu Rev Neurosci. 1996; 19:187–217. [PubMed: 8833441]

Luo M, Perkel DJ. Long-range GABAergic projection in a circuit essential for vocal learning. J Comp Neurol. 1999; 403:68–84. [PubMed: 10075444]

Luo M, Ding L, Perkel DJ. An avian basal ganglia pathway essential for vocal learning forms a closed topographic loop. J Neurosci. 2001; 21:6836–6845. [PubMed: 11517271]

Medina L, Reiner A. Do birds possess homologues of mammalian primary visual, somatosensory and motor cortices? Trends Neurosci. 2000; 23:1–12. [PubMed: 10631781]

Mello CV, Clayton DF. Song-induced ZENK gene expression in auditory pathways of songbird brain and its relation to the song control system. J Neurosci. 1994; 14:6652–6666. [PubMed: 7965067]

Mello CV, Clayton DF. Differential induction of the ZENK gene in the avian forebrain and song control circuit after metrazole-induced depolarization. J Neurobiol. 1995; 26:145–161. [PubMed: 7536234]

Mello CV, Ribeiro S. ZENK protein regulation by song in the brain of songbirds. J Comp Neurol. 1998; 393:426–438. [PubMed: 9550149]

Mello CV, Vicario DS, Clayton DF. Song presentation induces gene expression in the songbird forebrain. Proc Natl Acad Sci U S A. 1992; 89:6818–6822. [PubMed: 1495970]

Mello CV, Jarvis ED, Denisenko N, Rivas M. Isolation of song-regulated genes in the brain of songbirds. Methods Mol Biol. 1997; 85:205–217. [PubMed: 9276326]

Metzdorf R, Gahr M, Fusani L. Distribution of aromatase, estrogen receptor, and androgen receptor mRNA in the forebrain of songbirds and nonsongbirds. J Comp Neurol. 1999; 407:115–129. [PubMed: 10213192]

Nastiuk KL, Clayton DF. The canary androgen receptor mRNA is localized in the song control nuclei of the brain and is rapidly regulated by testosterone. J Neurobiol. 1995; 26:213–224. [PubMed: 7707043]

Nastiuk KL, Mello CV, George JM, Clayton DF. Immediate-early gene responses in the avian song control system: cloning and expression analysis of the canary c-jun cDNA. Brain Res Mol Brain Res. 1994; 27:299–309. [PubMed: 7898314]

Nottebohm F. The origins of vocal learning. Am Naturalist. 1972; 106:116–140.

Nottebohm F, Arnold AP. Sexual dimorphism in vocal control areas of the songbird brain. Science. 1976; 194:211–213. [PubMed: 959852]

Nottebohm F, Stokes TM, Leonard CM. Central control of song in the canary, *Serinus canarius*. J Comp Neurol. 1976; 165:457–486. [PubMed: 1262540]

Nottebohm F, Kelley DB, Paton JA. Connections of vocal control nuclei in the canary telencephalon. J Comp Neurol. 1982; 207:344–357. [PubMed: 7119147]

Ohara O, Gahara Y, Miyake T, Teraoka H, Kitamura T. Neurofilament deficiency in quail caused by nonsense mutation in neurofilament-L gene. J Cell Biol. 1993; 121:387–395. [PubMed: 8468353]

Price P. Developmenteal determinants of structure in zebra finch song. J Comp Physiol Psychol. 1979; 93:260–277.

Reiner A, Perkel DJ, Bruce LL, Butler AB, Csillag A, Kuenzel W, Medina L, Paxinos G, Shimizu T, Striedter G, Wild M, Ball GF, Durand S, Gunturkun O, Lee DW, Mello CV, Powers A, White SA, Hough G, Kubikova L, Smulders TV, Wada K, Dugas-Ford J, Husband S, Yamamoto K, Yu J, Siang C, Jarvis ED. Revised nomenclature for avian telencephalon and some related brainstem nuclei. J Comp Neurol. 2004; 473:377–414. [PubMed: 15116397]

Riters LV, Ball GF. Sex differences in the densities of alpha 2-adrenergic receptors in the song control system, but not the medial preoptic nucleus in zebra finches. J Chem Neuroanat. 2002; 23:269–277. [PubMed: 12048110]

Sakaguchi H, Saito N. The acetylcholine and catecholamine contents in song control nuclei of zebra finch during song ontogeny. Brain Res Dev Brain Res. 1989; 47:313–317.

Sakaguchi H, Saito N. Developmental change of cholinergic activity in the forebrain of the zebra finch during song learning. Brain Res Dev Brain Res. 1991; 62:223–228.

Sakaguchi T, Okada M, Kitamura T, Kawasaki K. Reduced diameter and conduction velocity of myelinated fibers in the sciatic nerve of a neurofilament-deficient mutant quail. Neurosci Lett. 1993; 153:65–68. [PubMed: 8510825]

Scharff C, Nottebohm F. A comparative study of the behavioral deficits following lesions of various parts of the zebra finch song system: implications for vocal learning. J Neurosci. 1991; 11:2896–2913. [PubMed: 1880555]

Schlinger BA, Arnold AP. Androgen effects on the development of the zebra finch song system. Brain Res. 1991; 561:99–105. [PubMed: 1797353]

Simpson HB, Vicario DS. Early estrogen treatment of female zebra finches masculinizes the brain pathway for learned vocalizations. J Neurobiol. 1991; 22:777–793. [PubMed: 1765783]

Sockman KW, Gentner TQ, Ball GF. Complementary neural systems for the experience-dependent integration of mate-choice cues in European starlings. J Neurobiol. 2004; 62:72–81. [PubMed: 15389683]

Soderstrom K, Tian Q, Valenti M, Di Marzo V. Endocannabinoids link feeding state and auditory perception-related gene expression. J Neurosci. 2004; 24:10013–10021. [PubMed: 15525787]

Sohrabji F, Nordeen EJ, Nordeen KW. Selective impairment of song learning following lesions of a forebrain nucleus in the juvenile zebra finch. Behav Neural Biol. 1990; 53:51–63. [PubMed: 2302141]

Spiro JE, Dalva MB, Mooney R. Long-range inhibition within the zebra finch song nucleus RA can coordinate the firing of multiple projection neurons. J Neurophysiol. 1999; 81:3007–3020. [PubMed: 10368416]

Teramitsu I, Kudo LC, London SE, Geschwind DH, White SA. Parallel FoxP1 and FoxP2 expression in songbird and human brain predicts functional interaction. J Neurosci. 2004; 24:3152–3163. [PubMed: 15056695]

Trojanowski JQ, Walkenstein N, Lee VM. Expression of neurofilament subunits in neurons of the central and peripheral nervous system: an immunohistochemical study with monoclonal antibodies. J Neurosci. 1986; 6:650–660. [PubMed: 2420946]

van der Gucht E, Vandesande F, Arckens L. Neurofilament protein: a selective marker for the architectonic parcellation of the visual cortex in adult cat brain. J Comp Neurol. 2001; 441:345–368. [PubMed: 11745654]

Vates GE, Broome BM, Mello CV, Nottebohm F. Auditory pathways of caudal telencephalon and their relation to the song system of adult male zebra finches. J Comp Neurol. 1996; 366:613–642. [PubMed: 8833113]

Vates GE, Vicario DS, Nottebohm F. Reafferent thalamo- “cortical” loops in the song system of oscine songbirds. J Comp Neurol. 1997; 380:275–290. [PubMed: 9100137]

Velho TA, Pinaud R, Rodrigues PV, Mello CV. Co-induction of activity-dependent genes in songbirds. Eur J Neurosci. 2005; 22:1667–1678. [PubMed: 16197507]

Verge VM, Tetzlaff W, Bisby MA, Richardson PM. Influence of nerve growth factor on neurofilament gene expression in mature primary sensory neurons. J Neurosci. 1990; 10:2018–2025. [PubMed: 2113088]

Wada K, Sakaguchi H, Jarvis ED, Hagiwara M. Differential expression of glutamate receptors in avian neural pathways for learned vocalization. J Comp Neurol. 2004; 476:44–64. [PubMed: 15236466]

Weaver IC, Cervoni N, Champagne FA, D’Alessio AC, Sharma S, Seckl JR, Dymov S, Szyf M, Meaney MJ. Epigenetic programming by maternal behavior. Nat Neurosci. 2004; 7:847–854. [PubMed: 15220929]

White SA. Learning to communicate. Curr Opin Neurobiol. 2001; 11:510–520. [PubMed: 11502400]

Wild JM. Neural pathways for the control of birdsong production. J Neurobiol. 1997; 33:653–670. [PubMed: 9369465]

Wild JM, Karten HJ, Frost BJ. Connections of the auditory forebrain in the pigeon (*Columba livia*). J Comp Neurol. 1993; 337:32–62. [PubMed: 8276991]

Yamasaki H, Bennett GS, Itakura C, Mizutani M. Defective expression of neurofilament protein subunits in hereditary hypotrophic axonopathy of quail. Lab Invest. 1992; 66:734–743. [PubMed: 1602743]

Zeigler, HP.; Marler, P. Behavioral neurology of birdsong. New York Academy of Sciences; New York: 2004. p. 788

Zhao Y, Szaro BG. Xefiltin, a new low molecular weight neuronal intermediate filament protein of *Xenopus laevis*, shares sequence features with goldfish gefiltin and mammalian alpha-internexin and differs in expression from XNIF and *NF-L*. J Comp Neurol. 1997; 377:351–364. [PubMed: 8989651]

Zopf D, Hermans-Borgmeyer I, Gundelfinger ED, Betz H. Identification of gene products expressed in the developing chick visual system: characterization of a middle-molecular-weight neurofilament cDNA. Genes Dev. 1987; 1:699–708. [PubMed: 3123320]

Zopf D, Dineva B, Betz H, Gundelfinger ED. Isolation of the chicken middle-molecular weight neurofilament (*NF-M*) gene and characterization of its promoter. Nucleic Acids Res. 1990; 18:521–529. [PubMed: 2106668]

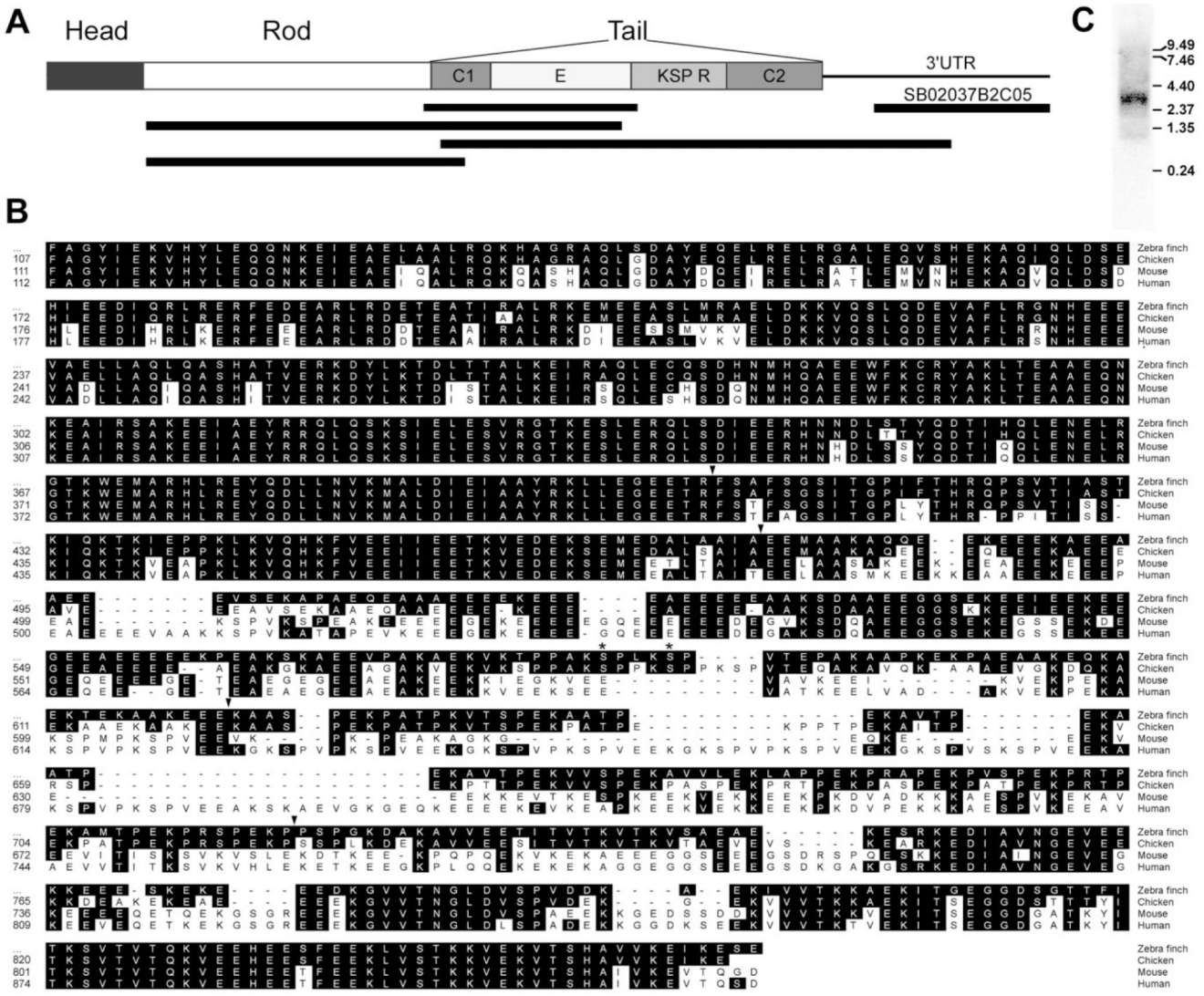

Fig. 1.

PCR cloning of the zebra finch *NF-M* homologue. **A:** Schematic representation of the organization of *NF-M* protein depicting its domains (head, rod, and tail), and tail subdomains. C1, conserved region 1; E, glutamic acid-rich region; R, repeats; C2, conserved region 2. Black bars indicate the relative position of the amplified fragments from which the sequence was derived. The black bar on the top right indicates the position of the clone from the ESTIMA collection. **B:** Alignment of the predicted amino acid sequence of zebra finch *NF-M* protein with homologues from other species. The numbers on the left indicate the relative position of residues in the respective sequences. Arrows indicate the transitions between the various domains. Asterisks indicate the presence of two conserved phosphorylation motifs (KSP). **C:** Northern blot of total zebra finch brain RNA hybridized with a ^{33}P-labeled *NF-M* antisense riboprobe. The molecular sizes of RNA markers (in kb) are indicated at right.

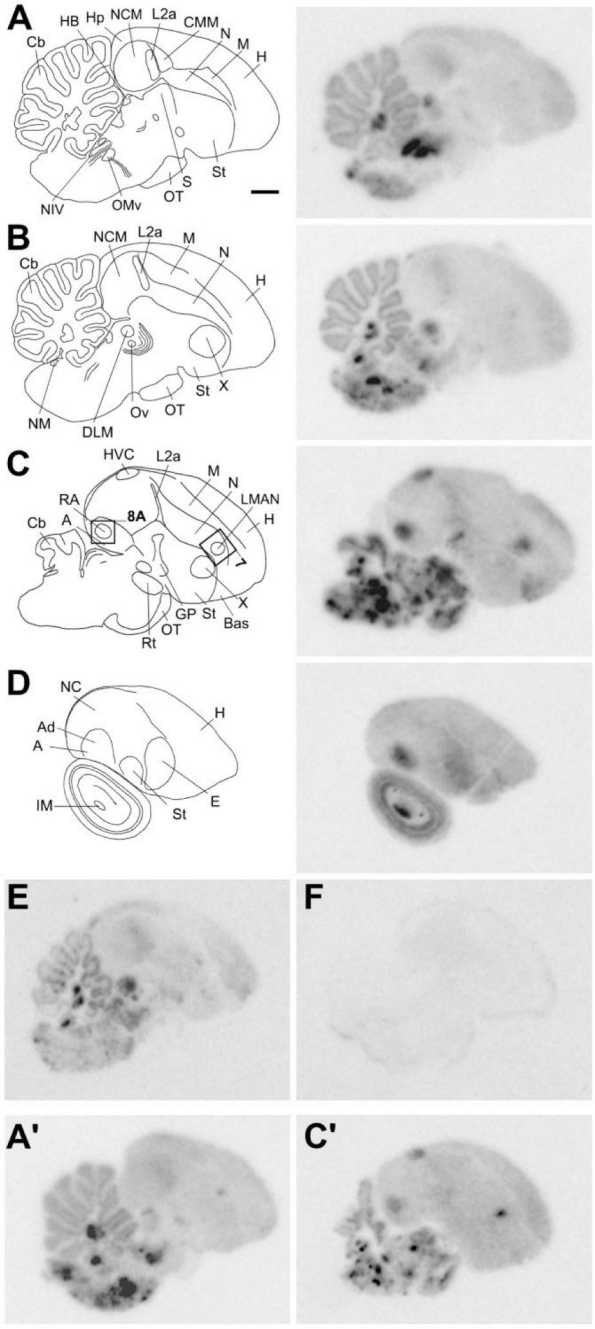

Fig. 2.

NF-M expression in serial parasagittal sections of a male zebra finch brain. Left panels in A–D: Camera lucida drawings of sections at ~0.4 mm (**A**), ~0.8 mm (**B**), ~1.8 mm (**C**), and ~3 mm (**D**) from the midline. Rectangles in C indicate the relative position of photomicrographs in Figures 7A and 8A. Right panels in A–D: Autoradiograms of the sections at the levels shown in the left panels, hybridized with the *NF-M* antisense riboprobe. **E,F:** Autoradiograms of adjacent brain sections at ~0.6 mm from the midline hybridized in parallel with antisense (E) or sense (F) strand riboprobes. **A′,C′:**

Autoradiograms of sections at levels similar to A and C, respectively, hybridized with antisense riboprobe for *NF-L*. For abbreviations see list. Scale bar = 1 mm.

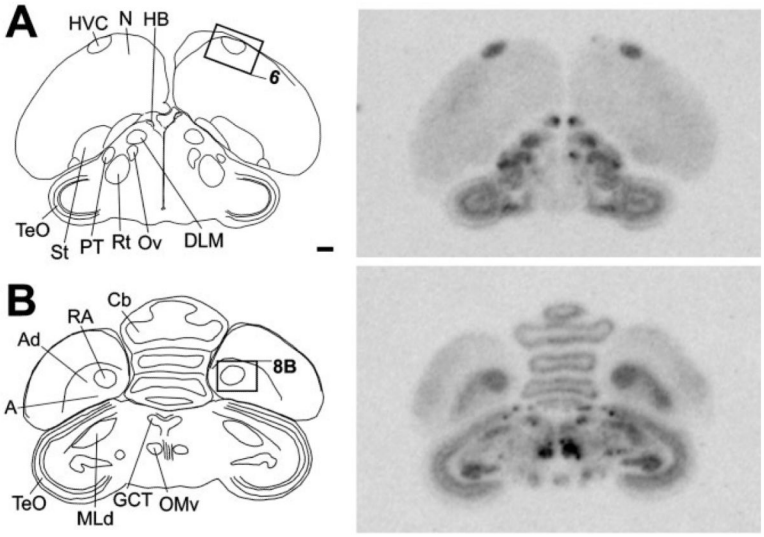

Fig. 3.

NF-M expression in frontal sections of a male zebra finch brain. Left panels: Camera lucida drawings of sections at the level of song nuclei HVC (**A**) and RA (**B**). Rectangles indicate the relative position of the photomicrographs shown on Figures 6 and 8B. Right panels: Autoradiograms of sections at the levels shown in the left panels, hybridized with the *NF-M* antisense riboprobe. For abbreviations see list. Scale bar = 1 mm.

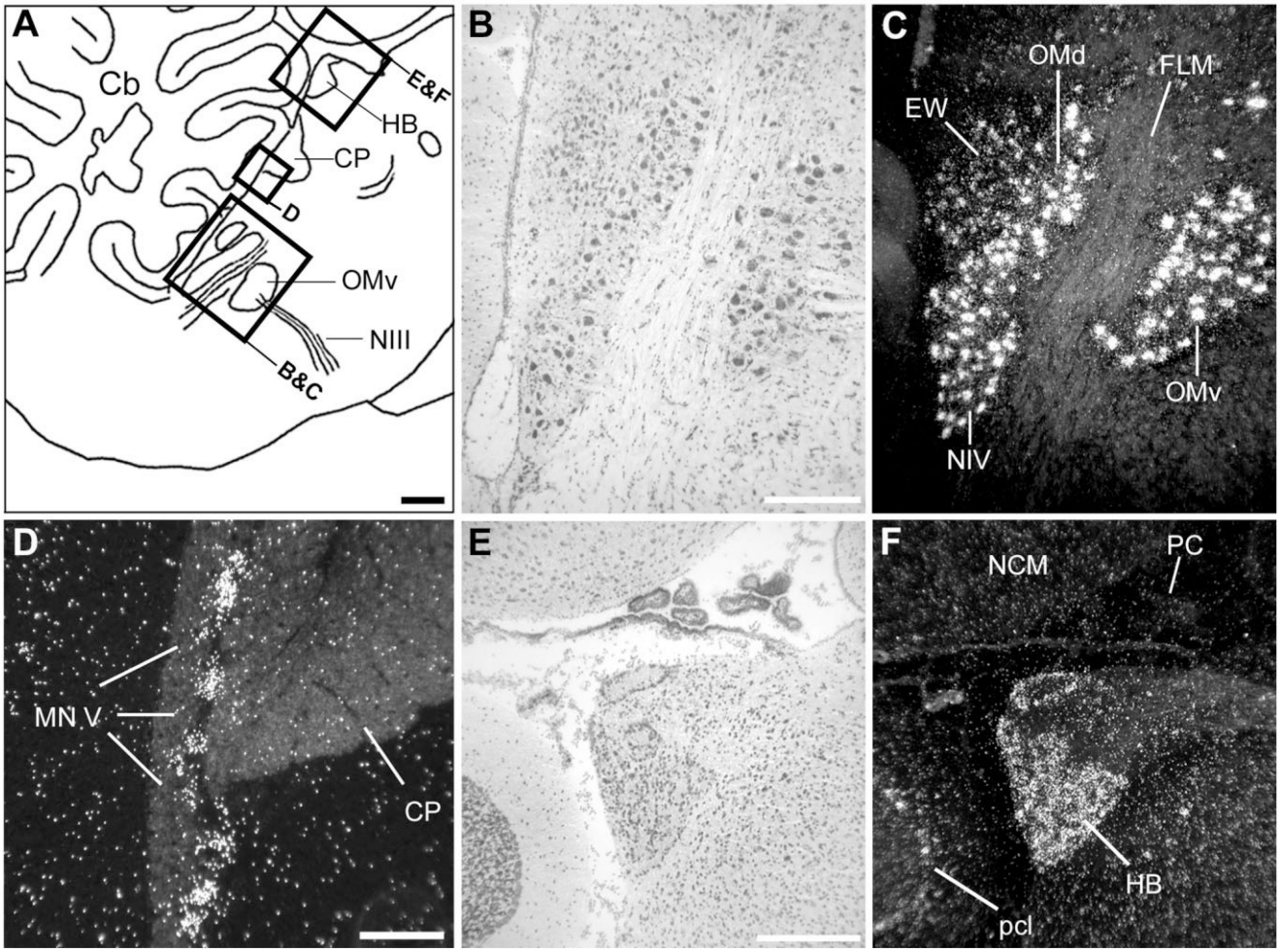

Fig. 4.

NF-M expression in cranial nerve nuclei and medial habenula. **A:** Camera lucida drawing of a parasagittal section depicting the regions in the medial brainstem and epithalamus (indicated by rectangles) shown in B–F. **B,C:** Brightfield view of Nissl staining and darkfield view of emulsion autoradiography depicting oculomotor and trochlear nerve nuclei. **D:** Darkfield view of emulsion autoradiography depicting the motor nucleus of the trigeminal nerve. **E,F:** Brightfield view of Nissl staining and darkfield view of emulsion autoradiography depicting the medial habenula and surrounds. The white signal indicates deposition of emulsion grains. In A, dorsal is upward and rostral is to the right. For abbreviations see list. Scale bars = 1 mm in A; 100 μm in B,D,E (apply to B–F).

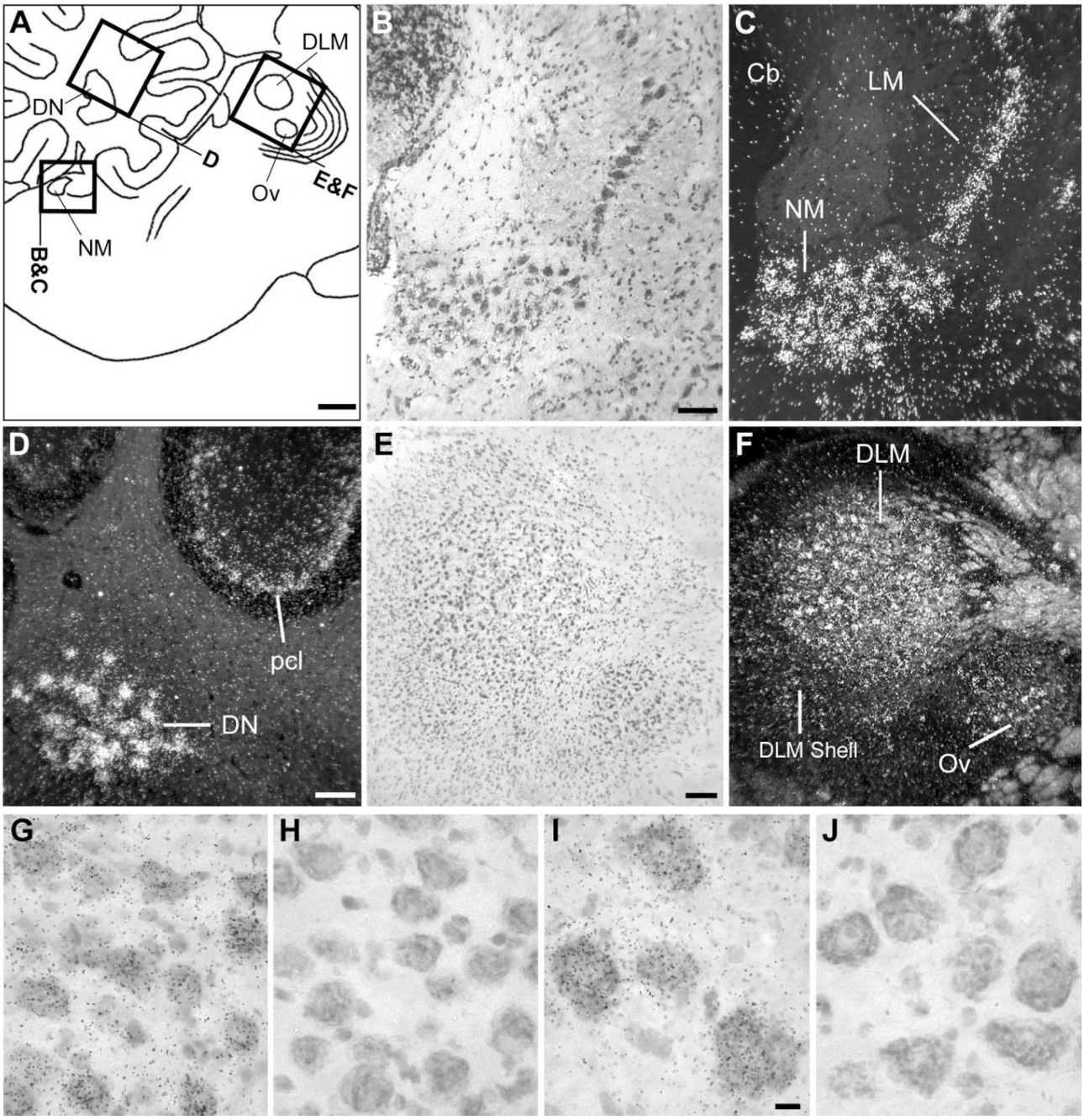

Fig. 5.

NF-M expression in the cochlear nucleus, thalamus, and cerebellum. **A:** Camera lucida drawing depicting the regions in the medial pons, cerebellum, and thalamus (indicated by rectangles) shown in B–F. **B,C:** Brightfield view of Nissl staining and darkfield view of emulsion autoradiography depicting cochlear nucleus NM and its target NL. **D:** Darkfield view of emulsion autoradiography depicting cerebellar structures. **E,F:** Brightfield view of Nissl staining and darkfield view of emulsion autoradiography depicting thalamic nuclei DLM and Ov. **G-J:** High-magnification brightfield view of emulsion autoradiography

depicting high expression levels in the large neuronal cells within the cochlear nucleus NM and the deep cerebellar nuclei (DN) in sections hybridized with the antisense riboprobe (G and I, respectively) and the lack of hybridization signal of the sense riboprobe in these same nuclei (H and J). In A, dorsal is upward and rostral is to the right. For abbreviations see list. Scale bars = 1 mm in A; 100 μm in B,D,E (apply to B–F); 10 μm in I (applies to G–J).

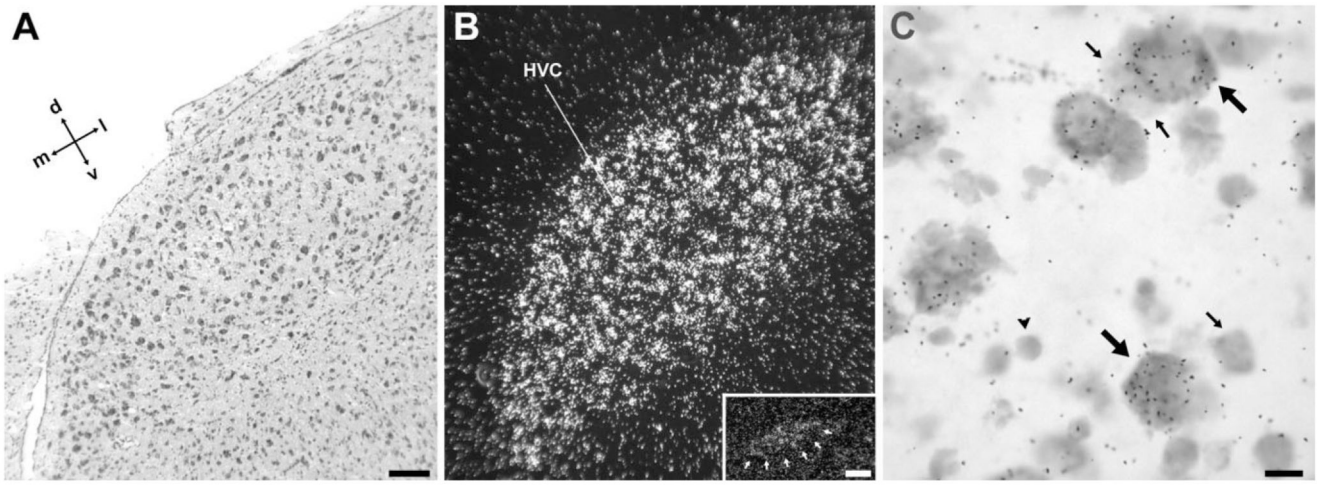

Fig. 6.

NF-M expression in song nucleus HVC. **A:** Detail brightfield view of a Nissl-stained frontal section through HVC, about the same level as in Figure 3A. **B:** Darkfield view of emulsion autoradiography at the same level as in A. **Inset:** Darkfield view of emulsion autoradiography of a medial parasagittal section at about 0.8 mm from the midline, showing expression in the para-HVC region. **C:** High-magnification view of labeled cells in HVC. Large arrows point to examples of large neuronal cells showing high *NF-M* expression levels; small arrows point to small neurons showing low or no expression; arrowhead depicts a glial-like cell lacking expression. For orientation see arrows in A. For the inset in B, dorsal is upward and rostral to the right. Scale bars = 100 μm in A (applies to A,B); 100 μm in inset; 10 μm in C.

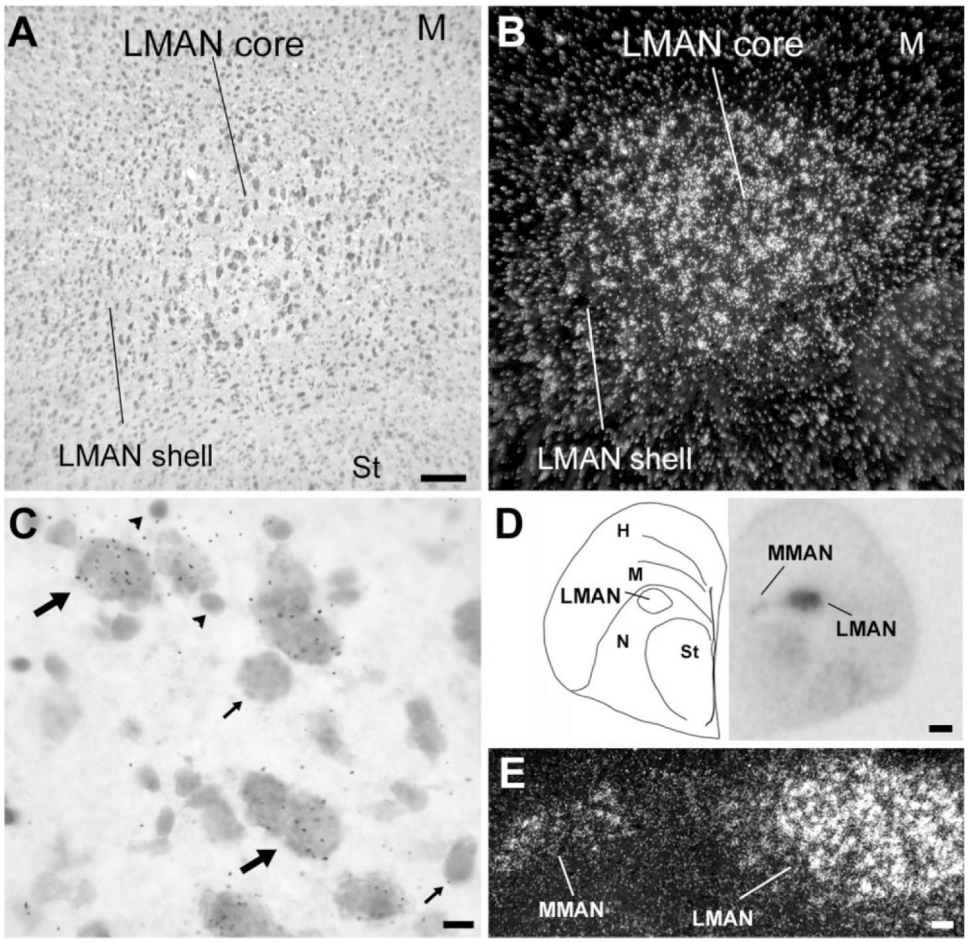

Fig. 7.

NF-M expression in song nuclei M- and LMAN. **A:** Detail brightfield view of a Nissl-stained parasagittal section through LMAN. **B:** Darkfield view of emulsion autoradiography at the same lavel as in A. **C:** High-magnification view of labeled cells in LMAN. Large arrows point to large neuronal cells with high accumulation of emulsion grains; small arrows point to smaller neuronal cells with no *NF-M* expression; arrowheads indicate glial-like cells lacking *NF-M* expression. **D:** Left panel: Camera lucida drawing of a frontal section at a level containing both M- and LMAN. Right panel: Autoradiogram of the section drawn in the left panel, indicating expression in both M- and LMAN. **E:** Detailed darkfield view of emulsion autoradiography of a section at the level shown in D, depicting *NF-M* expression in both M- and LMAN. For A–C, dorsal is upward and rostral is to the right; for E, dorsal is upward and medial is to the left. Scale bars = 100 μm in A (applies to A,B); 10 μm in C; 500 μm in D; 100 μm in E.

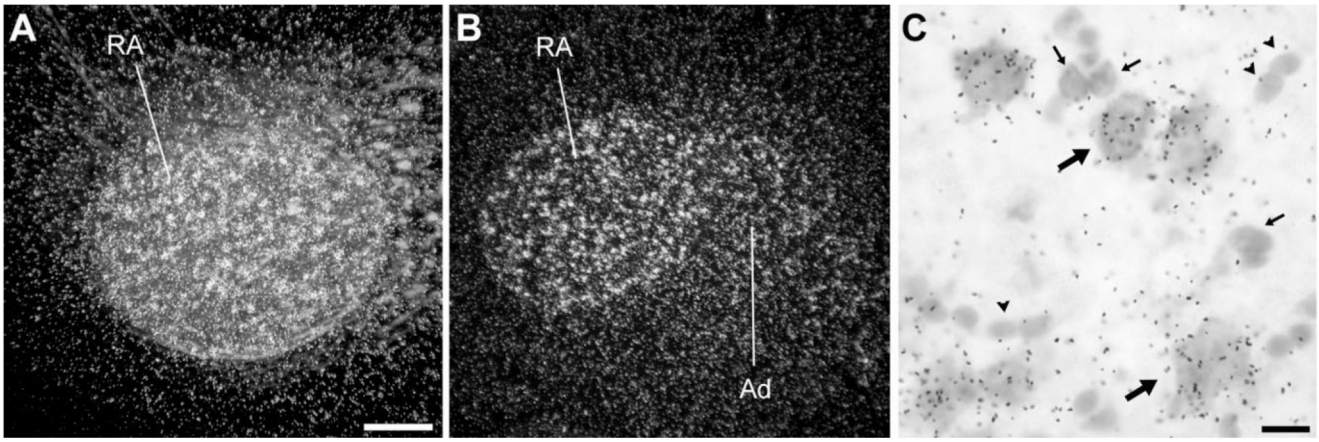

Fig. 8.

NF-M expression in song nucleus RA. **A,B:** Darkfield views of emulsion autoradiography of parasagittal (A) and frontal (B) sections through RA. **C:** High-magnification view of labeled cells in RA. Large arrows point to examples of large neuronal cells with high densities of emulsion grains; small arrows point to smaller neurons with low or no expression; arrowheads depict glial-like cells lacking *NF-M* expression. For A, dorsal is upward and rostral is to the right; for B, dorsal is upward and lateral to the right. Scale bars = 100 μm in A (applies to A,B); 10 μm in C.

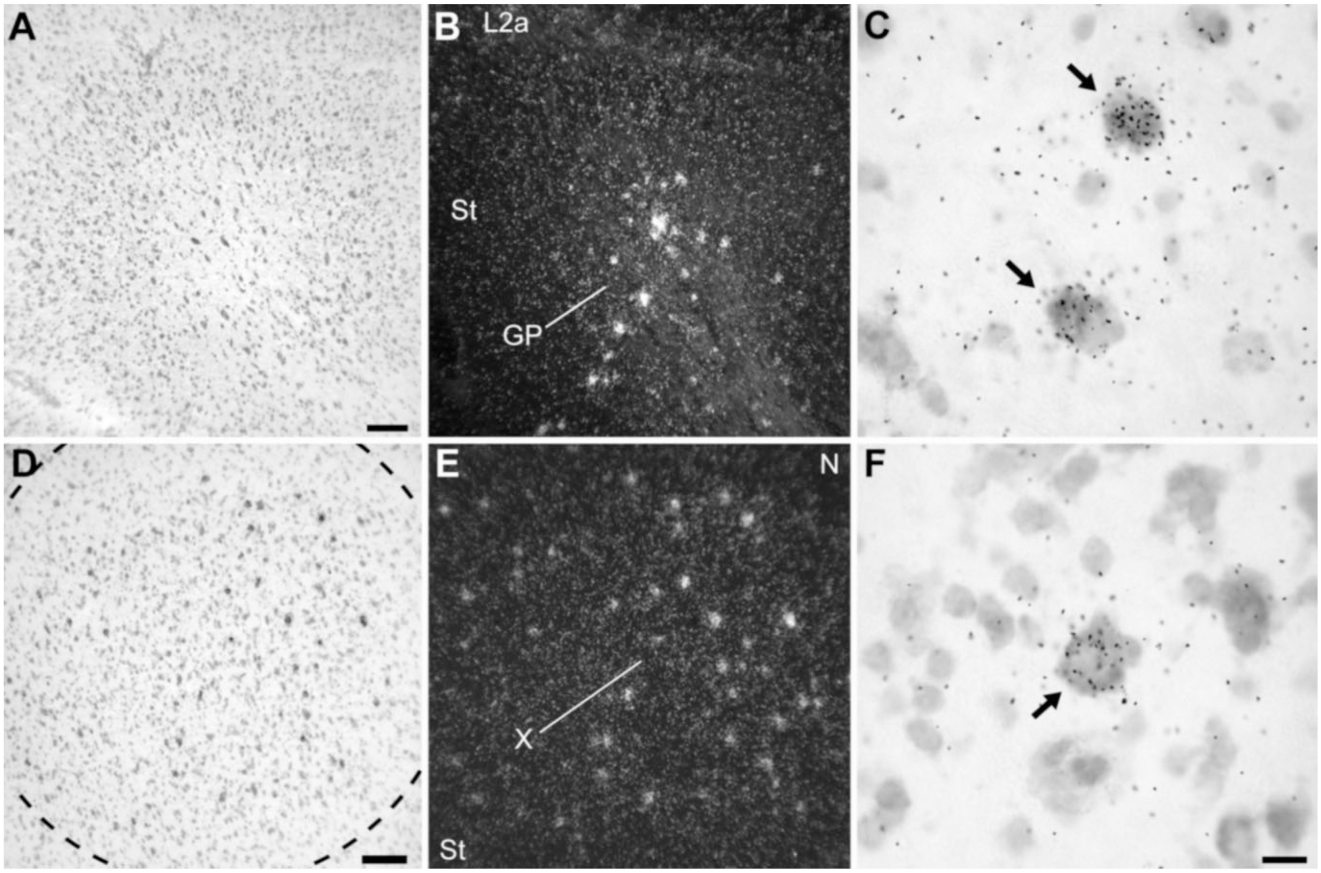

Fig. 9.

NF-M expression in the basal ganglia. **A,B:** Brightfield view of Nissl staining and darkfield view of emulsion autoradiography of parasagittal section depicting the caudal globus pallidus (GP), at about the same level as in Figure 2C. **C:** High-magnification view of labeled cells in GP. Arrows point to the sparse large neuronal cells with high accumulation of emulsion grains. **D,E:** Brightfield view of Nissl staining and darkfield view of emulsion autoradiography of frontal section through song nucleus area X in the medial striatum. **F:** High-magnification view of labeled cells within area X. Arrows point to widely spaced large neuronal cells with high accumulation of emulsion grains. For A–C, dorsal is upward and rostral is to the right; for D–F, dorsal is upward and lateral is to the right. For abbreviations see list. Scale bars = 100 μm in A (applies to A,B); 100 μm in D (applies to D,E); 20 μm in F (applies to C,F).

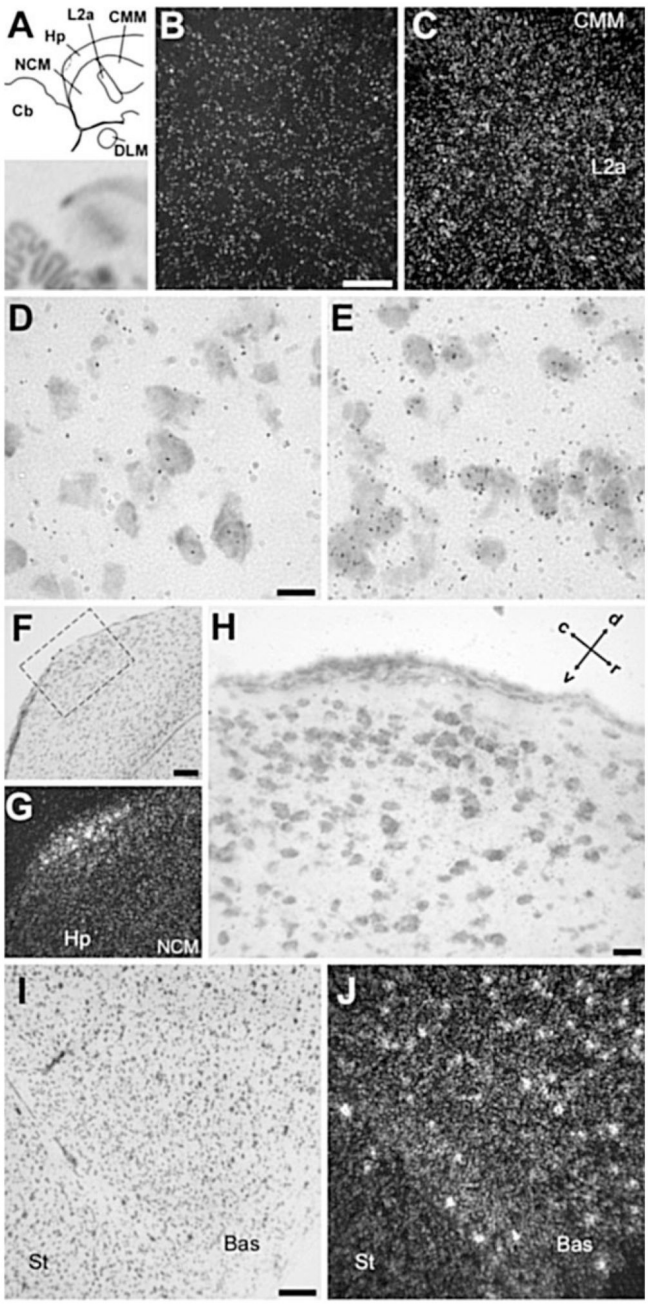

Fig. 10.

NF-M expression in the caudomedial and rostral telencephalon. **A:** Top panel: Camera lucida drawing of a parasagittal section through caudomedial auditory and hippocampal areas, at about the same level as in Figure 2B. Bottom panel: Autoradiography of the section drawn in the top panel. **B,C:** Detail darkfield views over NCM (B) and L2a (C) of emulsion autoradiography, depicting higher overall density of emulsion grains in L2a. **D,E:** Detail brightfield views of emulsion autoradiography over NCM (D) and L2a (E), depicting higher density of grains over cells in L2a. **F,G:** Detail brightfield view of Nissl staining and corresponding darkfield view of emulsion autoradiography depicting a small domain of

enriched expression in the caudodorsal hippocampus. **H:** Detailed brightfield view of Nissl-stained section depicting the caudodorsal hippocampal domain resembling a distinct nucleus and showing enriched *NF-M* expression (corresponds to the dashed rectangle in F). **I,J:** Brightfield view of Nissl staining and darkfield view of emulsion autoradiography depicting the nucleus basorostralis (Bas), at about the same level as in Figure 2C. For all panels except for H, dorsal is upward and rostral to the right; for H see arrows. For abbreviations see list. Scale bars = 100 μm in B (applies to B,C); 10 μm in D (applies to D,E); 100 μm in F (applies to F,G); 20 μm in H; 100 μm in I (applies to I,J).

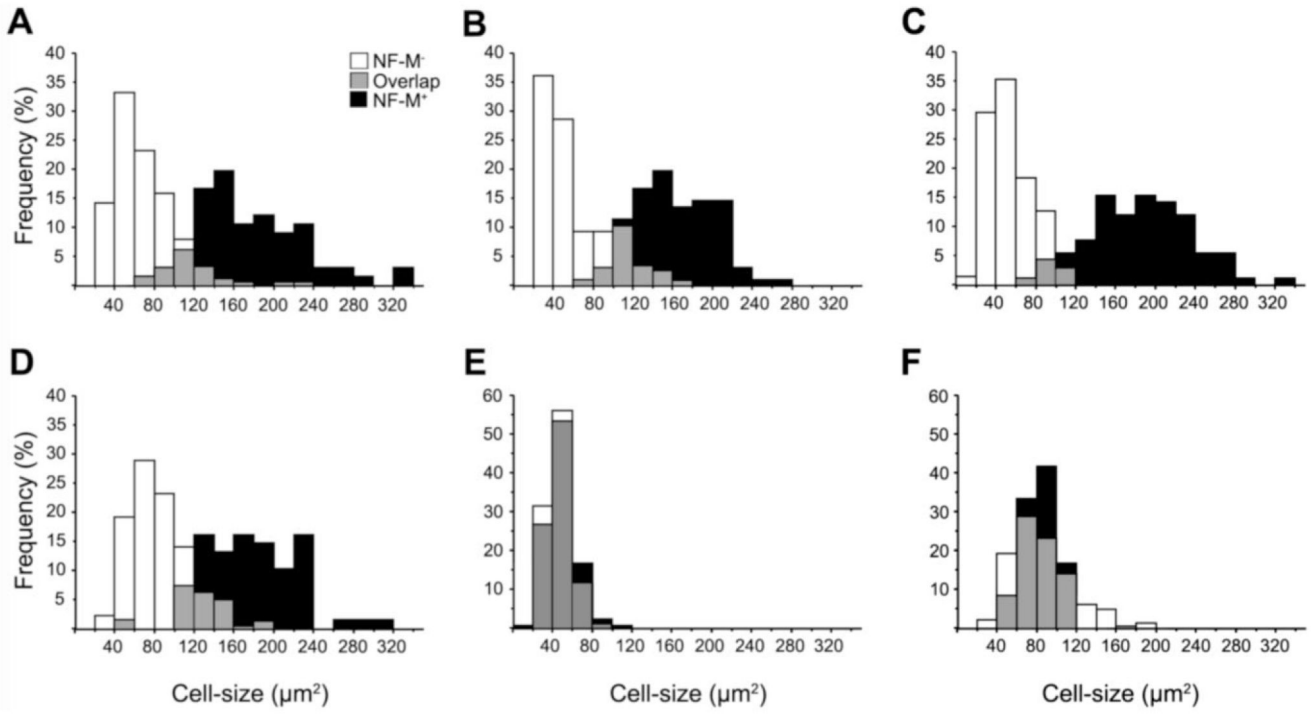

Fig. 11.

Cell-size distributions of *NF-M* positive (+) and negative (−) neurons. The graphs are relative frequency (%) histograms of *NF-M*$^+$ (black columns) and *NF-M*$^-$ (white columns) neurons ranked according to soma size in HVC (**A**), RA (**B**), LMAN (**C**), area X (**D**), L2a (**E**), and Hp (**F**). Gray columns represent the areas of overlap in the two distributions. The average soma sizes measured were (expressed as means ± SEM): for HVC, *NF-M*$^+$ = 175.3 ± 6.7 μm^2 (n = 66), *NF-M*$^-$ = 69.15 ± 2.25 μm^2 (n = 190); for LMAN, *NF-M*$^+$ = 185.0 ± 5.5 μm^2 (n = 92), *NF-M*$^-$ = 53.9 ± 2.7 μm^2 (n = 71); for RA, *NF-M*$^+$ = 161.9 ± 4.1 μm^2 (n = 119), *NF-M*$^-$ = 60.0 ± 3.0 (n = 96); for area X, *NF-M*$^+$ = 177.3 ± 5.7 μm^2 (n = 68), *NF-M*$^-$ = 48.2 ± 2.2 (n = 103); for L2a, *NF-M*$^+$ = 48.8 ± 0.9 μm^2 (n = 180), *NF-M*$^-$ = 46.5 ± 1.0 μm^2 (n = 184); and for Hp, *NF-M*$^+$ = 84.2 ± 4.9 μm^2 (n = 12), *NF-M*$^-$ = 85.0 ± 0.9 μm^2 (n = 219). For abbreviations see list.

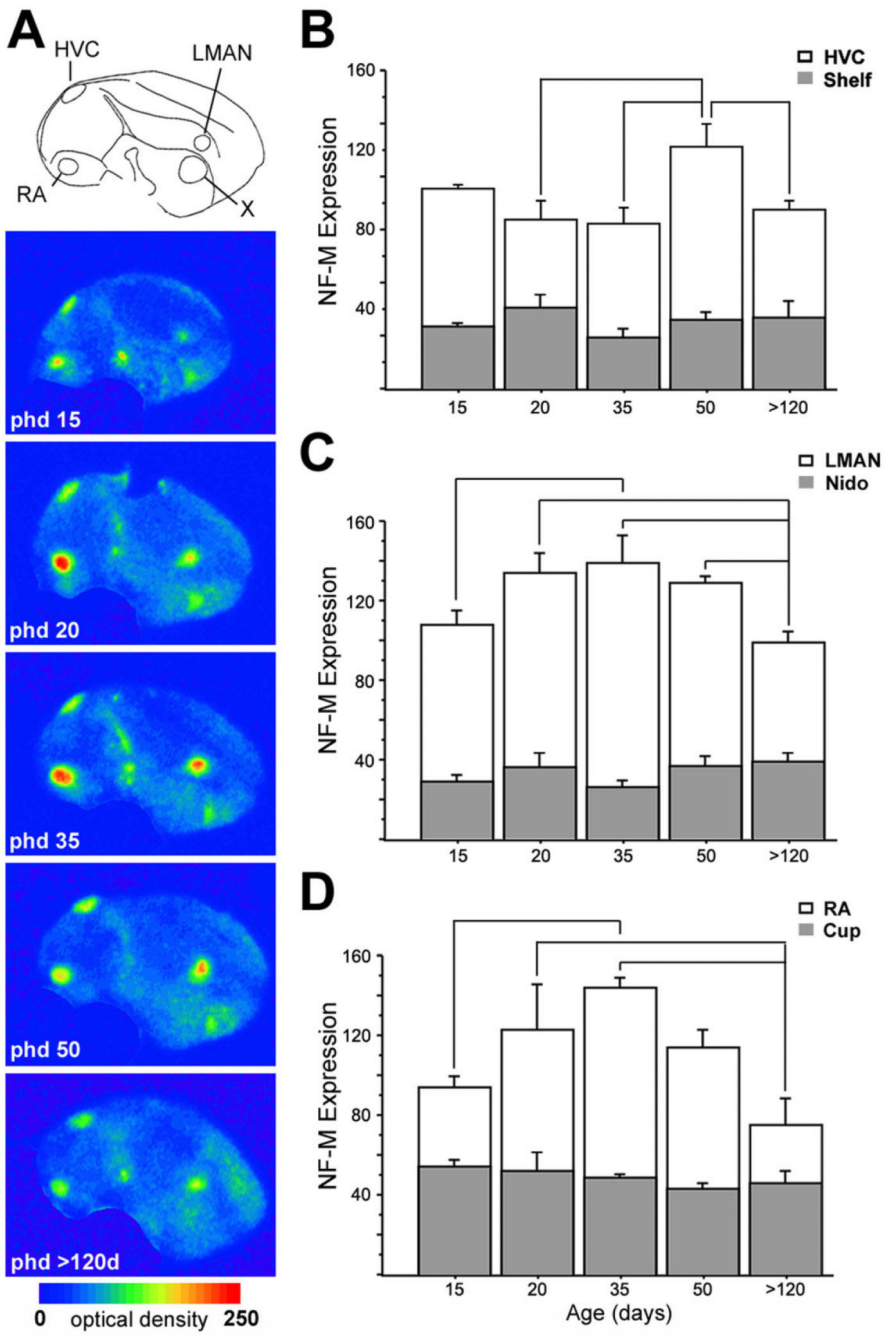

Fig. 12.

Changes in *NF-M* expression in song control nuclei during development. **A:** Color-coded phosphorimager autoradiograms of parasagittal sections from males of different ages (in days posthatch), at levels containing all pallial song control nuclei, as indicated by camera lucida drawing at top. **B-D:** Densitometric analysis of *NF-M* expression (in O.D.) in HVC, LMAN, and RA (white columns) and adjacent regions in the nido- and arcopallium (gray columns), as a function of age (in days posthatch). Depicted are means ± SEM; significant differences are indicated by lines. For abbreviations see list.

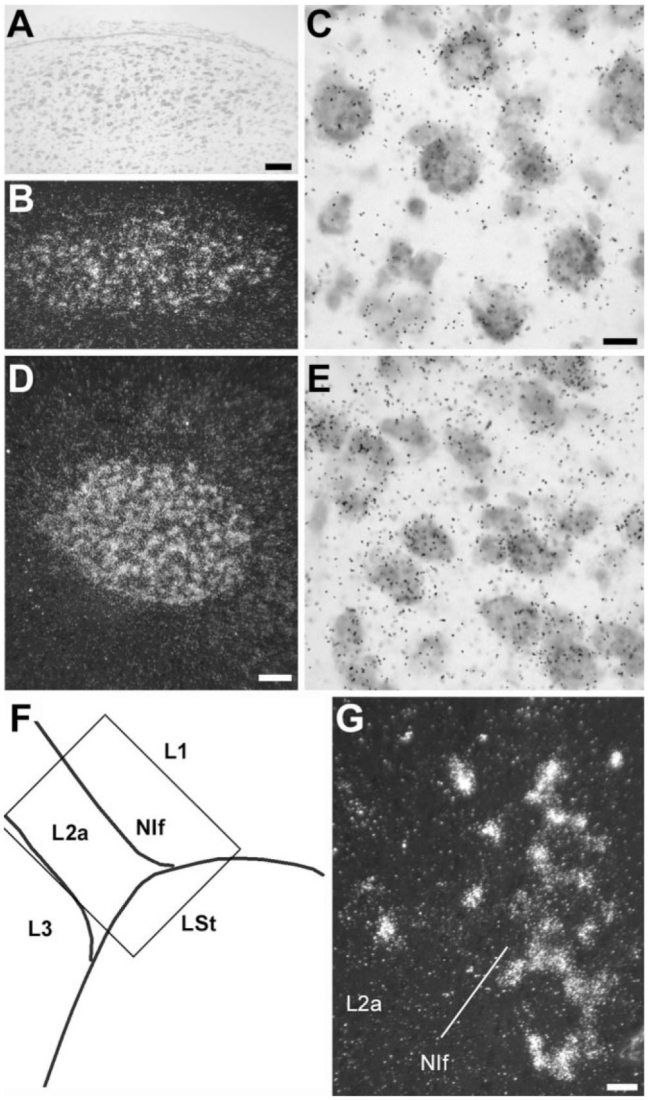

Fig. 13.

NF-M expression in song control nuclei of juvenile males. **A:** Brightfield view of Nissl staining depicting HVC on phd 20. **B,D:** Darkfield views of emulsion autoradiograms depicting HVC (B, same field as in A) and RA (D) on phd 20. **C,E:** High-magnification views depicting accumulation of emulsion grains over large neuronal cells in HVC (C) and RA (E) of a 20-day-old bird; notice the higher cell density compared with adult RA in Figure 8C. **F:** Camera lucida drawing of parasagittal section depicting NIf and adjacent field L subdivisions in a 35-day-old bird (at a level more medial than in Fig. 11A). The area depicted by the rectangle is shown in G. **G:** Darkfield view of emulsion autoradiogram of section through NIf and adjacent field L2a, depicting accumulation of labeled cells in NIf. Dorsal is upward and rostral to the right. For abbreviations see list. Scale bars = 100 μm in A (appplies to A,B); 10 μm in C (applies to C,E); 100 μm in D; 20 μm in G.

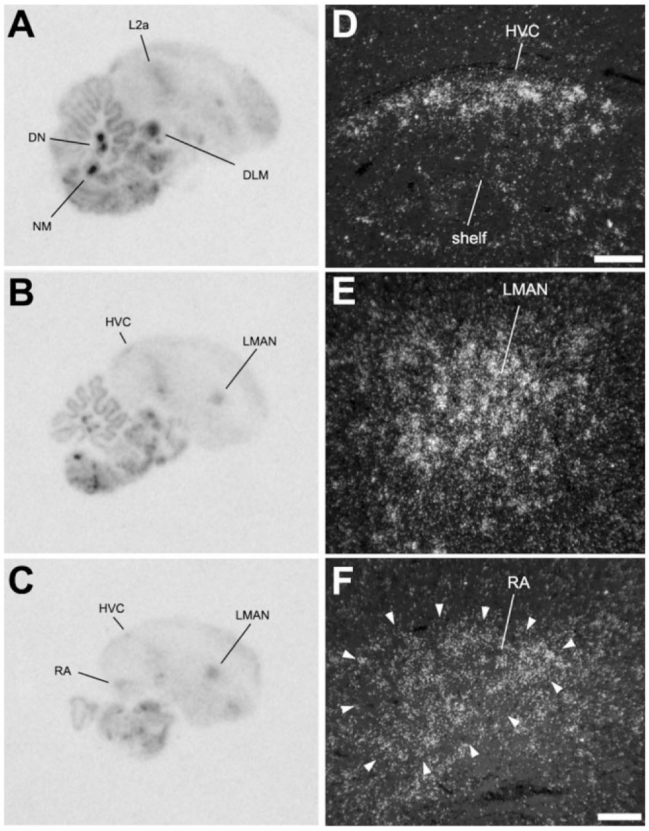

Fig. 14.

NF-M expression in parasagittal sections of a female zebra finch brain. **A-C:** Phosphorimager autoradiograms of sections at ~0.8 mm (A), ~1.3 mm (B), and ~1.8 mm (C) from the midline, hybridized with the *NF-M* antisense riboprobe. **D-F:** Darkfield view of emulsion autoradiography depicting the female HVC (D), LMAN (E), and RA (F). Arrowheads in F indicate the cytoarchitectonic boundaries of RA. Scale bars = 100 μm.

TABLE 1

Relative Expression Levels[1] of NF-M in Zebra Finch Brain Structures[2]

Cerebellum		
DN		+ + + + +[1]
gl		+
ml		+
Pcl		+ + + +
Diencephalon		
DLM		+ + +
HB		+ + + +
Ov		+ + +
Rt		+ + + + +
Medulla		+ + +
Midbrain		
EW		+ + +
IM		+ + + + +
NIV		+ + + + +
OM		+ + + + +
Pt		+ + +
TeO		+ + +
Pons		
MN V		+ + + + +
NL		+ + + + +
NM		+ + + + +
Telencephalon		
Arcopallium		+
	RA	+ + + +
	Ad	+ + +
Basorostralis		+ +
Entopallium		+ +
Globus pallidus		+ + + +
Hippocampus		+
	Hp (caudal)	+ + +
Hyperpallium		+ +
Mesopallium		+
	CMM	+
Nidopallium		+
	NCM	+
	L2a	+ +
	LMAN	+ + + +
	MMAN	+ + +
	HVC	+ + + +

	Nlf	+ + +
Septum		+
Striatum		+
	Area X	+

[1] Semi-quantitative scale based on the visual inspection of signal density in both phosphorimager and emulsion autoradiography.

[2] Structures are listed alphabetically; for abbreviations, see list.